Journal of Statistical Physics, Vol. 44, Nos. 5/6, 1986

Finite-Size Scaling Analysis of the Φ^4 Field Theory on the Square Lattice

A. Milchev,[1,2] D. W. Heermann,[1] and K. Binder[1]

Received November 20, 1985; final May 5, 1986

Monte-Carlo calculations are performed for the model Hamiltonian $\mathcal{H} = \sum_i [(r/2)\,\Phi^2(i) + (u/4)\,\Phi^4(i)] + \sum_{\langle ij \rangle} (C/2)[\Phi(i) - \Phi(j)]^2$ for various values of the parameters r, u, C in the crossover region from the Ising limit ($r \to -\infty$, $u \to +\infty$) to the displacive limit ($r = 0$). The variable $\phi(i)$ is a scalar continuous spin variable which can lie in the range $-\infty < \phi(i) < +\infty$, for each lattice site (i). $\phi(i)$ is a priori selected proportional to the single-site probability in our Monte Carlo algorithm. The critical line is obtained in very good agreement with other previous approaches. A decrease of apparent critical exponents, deduced from a finite-size scaling analysis, is attributed to a crossover toward mean-field values at the displacive limit. The relation of this model to the coarse-grained Landau–Ginzburg–Wilson free-energy functional of Ising models is discussed in detail, and, by matching local moments $\langle \Phi^2(i) \rangle$, $\langle \Phi^4(i) \rangle$ to corresponding averages of subsystem blocks of Ising systems with linear dimensions $l = 5$ to $l = 15$, an explicit construction of this coarse-grained free energy is attempted; self-consistency checks applied to this matching procedure show qualitatively reasonable behavior, but quantitative difficulties remain, indicating that higher-order terms are needed for a quantitatively satisfactory description.

KEY WORDS: Continuous Ising model; order–disorder; displacive; Monte-Carlo simulation; finite-size scaling; critical exponents.

1. INTRODUCTION

Since the pioneering work of Kadanoff[1] and Wilson[2] it is well-established that the comon features of the behavior displayed by various

[1] Institut für Physik, Johannes-Gutenberg-Universität Mainz, D-6500 Mainz, Postfach 3980, Federal Republic of Germany.

[2] Alexander-von-Humboldt fellow. Permanent address: Institute for Physical Chemistry, Academy of Sciences, Sofia, Bulgaria.

0022-4715/86/0900-0749$05.00/0

systems near their critical point reflect a deeper universality in the spectrum of configurations, coarse-grained to eliminate system-specific microscopic details. This coarse-graining procedure, as discussed by many authors,[1,3–10] may be carried out by dividing the system into "cells" or "blocks" of linear dimension l, where l exceeds microscopic lengths (lattice spacing or interaction range) but is smaller than the correlation length ξ. Instead of the microscopic Hamiltonian of the system, one then studies, rather, the "coarse-grained Helmholtz free-energy functional"[5,10] (also called "Ginzburg–Landau–Wilson Hamiltonian" $\mathscr{H}_{\mathrm{GLW}}$) or the related coarse-grained, order-parameter, probability density function.[6–9] The latter quantity often is considered in the context of computer simulations, where it is analyzed to obtain critical properties[6,7,11] and locate (first-order) phase boundaries.[12] The coarse-grained free energy forms the basis of theoretical approaches to numerous problems, including spinodal decomposition and nucleation,[3,4,10] wetting,[13] the surface tension and interface profile of gas–liquid and liquid–liquid interfaces,[14] and, last but not least, the starting point for the renormalization group theory of critical phenomena.[2,15,16]

However, despite its crucial conceptual importance, the explicit relationship between the microscopic Hamiltonian and the associated Ginzburg–Landau–Wilson Hamiltonian is hardly ever worked out. Let us discuss this problem for the Ising Hamiltonian on d-dimensional cubic lattices ($d = 2, 3, 4$) of lattice spacing a

$$\mathscr{H}_{\mathrm{Ising}} = -\sum_{k \neq k'} J_{kk'} S_k S_{k'} \tag{1}$$

where spins $S_k = \pm 1$ are located on the lattice sites and interact with exchange couplings $J_{kk'}$ in zero external field. Dividing the lattice into cubic blocks of linear dimensions l, we define a block coordinate $\phi_l(\vec{x})$ as

$$\Phi_l(i) = (1/l^d) \sum_{k \in i\text{th cell}} S_k \tag{2}$$

Note that the block center of gravity is denoted by $\vec{x}$, and we may consider the block coordinate Φ_l either for a continuum of sites $\{\vec{x}\}$ or again as a regular lattice of sites $\{i\}$ (with rescaled lattice spacing–the original lattice spacing is taken as unity).

Now it is *assumed* that the Boltzmann factor $P(\{S_k\})$

$$P(\{S_k\}) = (1/Z) \exp\{-\mathscr{H}_{\mathrm{Ising}}/k_B T\} \tag{3a}$$

which describes the probability that a configuration $\{S_k\}$ occurs in thermal equilibrium, can essentially be replaced by [for $J_{kk'}$ being ferromagnetic]

$$P(\{\Phi_l(i)\}) = \frac{1}{Z} \exp[-\mathcal{H}_{\mathrm{GLW}}\{\Phi_l(i)\}] \tag{3b}$$

The Ginzburg–Landau–Wilson Hamiltonian for the case of a lattice of discrete sites $\{i\}$ is given by

$$\mathcal{H}_{\mathrm{GLW}}\{\Phi_l(i)\} = l^d \sum_i \left[\frac{1}{2} r_l \Phi_l^2(i) + \frac{1}{4} u_l \Phi_l^4(i) + \frac{1}{6} v_l \Phi_l^6(i) + \cdots\right] + \frac{1}{2} l^d \sum_{\langle ij \rangle} C_l [\Phi_l(i) - \Phi_l(j)]^2 / l^2 + \cdots \tag{4a}$$

where $\langle i, j \rangle$ denotes a sum over nearest-neighbor pairs on the lattice formed by the cells, while for the continuum case, $\mathcal{H}_{\mathrm{GLW}}\{\Phi(\vec{x})\}$ is given by

$$\mathcal{H}_{\mathrm{GLW}}\{\Phi(\vec{x})\} = \int d\vec{x} \left[\frac{1}{2} r_l' \Phi_l^2(\vec{x}) + \frac{1}{4} u_l' \Phi_l^4(\vec{x}) + \frac{1}{6} v_l' \Phi_l^6(\vec{x}) + \cdots + \frac{1}{2} C_l' (\nabla \Phi_l(\vec{x}))^2 + \cdots\right] \tag{4b}$$

The factor $(k_B T)^{-1}$ in eq. (3a) has been absorbed in the coefficients r_l, u_l, v_l, C_l or r_l', u_l', v_l', C_l',..., respectively.

Now, it is rather generally believed that the universal critical behavior of the models eqs. (1, 4) is identical, apart from short wave length properties which are still contained in eq. (1), (3a) but are sacrificed by the coarse-graining procedure which leads to eqs. (3b, 4). This should not matter since the short wavelength behavior should be irrelevant at criticality, although this universality has been occasionally questioned.[17,18] However, even if one accepts that eqs. (1), (4) belong to the same—Ising—universality class, there remain a number of questions:

(i) What is the precise correspondence between the couplings $J_{kk'}/k_B T$ of the original model and the coupling constants r_l, u_l, v_l, C_l,... of its coarse-grained version?

(ii) For which range of temperatures around T_c is the mapping of eq. (1) to eq. (4) accurate?

(iii) Is it a good approximation to reduce $\mathcal{H}_{\mathrm{GLW}}$ to the Φ^4 field theory from the outset [omitting the term $v_l \Phi_l^6$ and higher-order terms, as well as higher-order gradient terms in eq. (4b)? Renormalization group theory[15] shows that these terms are irrelevant to the universal

critical behavior near $d=4$ dimensions, but they yield corrections to scaling and thus limit the asymptotic critical region.

(iv) If the interactions $J_{kk'}$ are (at least partially) antiferromagnetic, eq. (1) may lead to critical behavior belonging to several different universality classes, e.g., the XY model with cubic anisotropy,[19] in which case $\mathscr{H}_{\mathrm{GLW}}$ has a qualitatively different structure involving a vector field $\vec{\Phi}_l(\vec{x})$ rather than the scalar field involved here. The question then arises, for a given set of interactions $\{J_{kk'}\}$, how to clarify the appropriate structure of $\mathscr{H}_{\mathrm{GLW}}$.

(v) For studying universal critical phenomena we wish to consider a coarse-graining satisfying $1 \ll l \ll \xi$, with l staying finite at T_c where ξ diverges. Then, near T_c one can assume that u_l and C_l are temperature-independent positive constants while r_l has a regular temperature dependence, $r_l \approx \hat{r}_l(T - T_c^{\mathrm{MF}})/T$, T_c^{MF} being the critical temperature of the mean-field approximation applied to eq. (4). For other applications of the coarse-grained free-energy functional, however, such as spinodal decomposition,[3,4,10] one wishes to have $l \approx \xi$. Then the coefficients r_l, u_l, v_l, C_l,... in eq. (4) must get a singular temperature-dependence, about which relatively little[5-9] is known.

Attempts to address some of these questions have been made by Bruce[8,9] on the basis of approximate recursion relations[2] and by Monte-Carlo methods.[6,7] In principle, by Monte-Carlo study of an Ising model one could sample $P_l(\{\Phi(i)\})$ and then reconstruct the appropriate $\mathscr{H}_{\mathrm{GLW}}\{\Phi_l(i)\}$. In practice, however, such a program is prohibitively difficult; hence, so far, instead of the full distribution function $P_l\{\Phi_l(i)\}$, which is a function of *all* block magnetizations, only the *reduced* distribution function $p_l(\Phi_l)$ of a single subsystem block[6,7] or of two neighboring subsystem blocks $p_l'[\Phi_l(i), \Phi_l(j)]$ have been obtained,[7] all other block magnetizations being averaged over. From this work, rough guesses of the coefficients r_l, u_l could be obtained[7] as a function of the coupling constant J/T in the vicinity of the critical temperature in a three-dimensional nearest-neighbor Ising model. However, C_l can hardly be obtained reliably in this manner.

In the present paper, we are again studying the relation between the microscopic and the coarse-grained Hamiltonian with Monte-Carlo methods, but with the approach (complementary to Refs. 6, 7) to study directly the Φ^4 model [eq. (4a) with $v_l=0$ and all higher-order terms omitted]. We obtain both global (collective) properties of this model as a function of its parameters r_l, u_l, C_l [the index l henceforth being omitted], as well as local ones, such as the single (block-)site probability distribution

$p[\Phi(i)]$ and its moments. We then can elucidate the mapping from $\mathscr{H}_{\text{Ising}}$ to $\mathscr{H}_{\text{GLW}}$ by comparing the present $p[\Phi(i)]$ with the $p_l[\Phi_l(i)]$ of the Ising model, obtained previously for various block sizes l.[6]

Apart from the interest from the point of view of coarse-graining, the Φ^4 model on a lattice [remember that Φ_i can adopt any real value, $-\infty < \Phi(i) < +\infty$]

$$\mathscr{H}_{\Phi^4} = \sum_i \left[\frac{r}{2} \Phi^2(i) + \frac{u}{4} \Phi^4(i) \right] + \sum_{\langle ij \rangle} \frac{C}{2} [\Phi(i) - \Phi(j)]^2 \tag{5}$$

is also of great interest as a microscopic model of structural transitions[20–29] (in particular, the case $d=2$ is a model for surface reconstruction.[28,29]). Equation (5) has been studied as the prototype model displaying crossover from the "order-disorder" limit [for C fixed but $u \to \infty$, $r \to -\infty$, eq. (5) becomes a nearest-neighbor Ising model[20,23]] to the "displacive" limit [for $r \to 0$, C, u fixed the phase transition is depressed to zero temperature and the critical behavior is Gaussian.[20,23] Hence we discuss our work in the context of this problem, too, and compare our numerical results to related previous calculations[22,24,28,30,31] whenever possible.

In Section 2 we give a brief reformulation of the model eq. (5), exploiting the well-known fact[24,26,28] that one of the three parameters r, u, C is redundant and can be absorbed by rescaling the field Φ_i; this also serves to make the relation to previous work more explicit. In Section 3 we describe our Monte-Carlo procedure and in Section 4 we present our "raw data" for various lattice sizes on the square lattice. Temperature-dependence of $\langle \Phi(i)^2 \rangle$ and of $\langle \Phi_l^2(i) \rangle$ for Ising models with various l and dimensionalities is discussed in Section 5 in view of the interest in this quantity, since the analogous local density fluctuation $\langle \rho^2 \rangle_{\text{loc}} - \langle \rho \rangle^2$ is deduced from vibrational Raman spectra of N_2 near the gas–liquid critical point[32] and recent confusion on the theoretical interpretation of this quantity.[33] Section 6 gives a preliminary discussion of the critical behavior of the model eq. (5) by finite-size scaling methods,[34] similar to previous applications to Ising problems.[35,36] However, our Monte-Carlo data are far too rough to settle the issue of whether a violation of universality occurs;[18,37] rather, they show the limitation of finite-size scaling analyses of Monte-Carlo data in a crossover region. Finally, Section 7 turns to the problem of constructing the direct correspondence between the nearest-neighbor Ising model and the corresponding coarse-grained free energy near criticality, while Section 8 summarizes our conclusions and gives an outlook for future work.

2. MEAN-FIELD APPROXIMATION AND RESCALINGS OF THE MODEL

In the mean-field approximation (MFA) possible spatial fluctuations of the order parameter are neglected, and hence the second sum on the right-hand-side of eqs. (4a, 5) can be neglected in the partition sum $Z = \mathrm{Tr}\{\Phi(i)\} \exp[-\mathscr{H}_{\Phi^4}]$. This means that for $r<0$ ($T<T_c^{\mathrm{MF}}$), the free energy is minimized by two homogeneously ordered phases with order parameter $\bar{\Phi}_{\mathrm{MF}}$,

$$\bar{\Phi}_{\mathrm{MF}} = \pm(-r/u)^{1/2} \tag{6}$$

while $\bar{\Phi}_{\mathrm{MF}} \equiv 0$ for $r \geqslant 0$ ($T \geqslant T_c^{\mathrm{MF}}$). If we add a term involving a wave-vector dependent field to eq. (5), $-\Sigma\Phi(i)\, h \cos(\vec{q}\cdot\vec{r}_i)$, and treat the resulting perturbation of the homogeneous state eq. (6) in linear response, we find the wave-vector dependent susceptibility $\chi_{\mathrm{MF}}(\vec{q})$

$$\chi(\vec{q}) = \chi_{\mathrm{MF}}/(1+q^2\xi_{\mathrm{MF}}^2), \qquad \chi_{\mathrm{MF}} = (-2r)^{-1}, \qquad \xi_{\mathrm{MF}} = [C/(-2r)]^{1/2} \tag{7}$$

The mean-field approximation becomes valid if the correlation length amplitude tends to infinity; i.e., the parameter $C \to \infty$, with r and u keeping fixed (this corresponds to the case of long-range forces), or $r \to 0$, with C and u fixed (the displacive limit).

One possible rescaling of $\mathscr{H}_{\Phi^4}$ is obtained by normalizing Φ with the mean-field order parameter, i.e., in terms of $m(i) \equiv \Phi(i)/\bar{\Phi}$, which yields

$$\mathscr{H}_{\Phi^4} = \frac{r^2}{u}\left\{\sum_i \left[-\frac{m^2(i)}{2}+\frac{m^4(i)}{4}\right] + \xi_{\mathrm{MF}}^2 \sum_{\langle ij\rangle} [m(i)-m(j)]^2\right\} \tag{8}$$

This normalization is essentially the choice of Ref. 24. We can identify the parameters K, L (we denote L henceforth as $\tilde{L}$ to avoid confusion with the lattice size) of Ref. 24 as $K = -rC/u = 2(r\xi_{\mathrm{MF}})^2/u$, $\tilde{L} = r^2/4u$. $\tilde{L} \to \infty$ corresponds to the Ising limit, $\tilde{L} \to 0$ to the displacive limit. [Similarly, we can identify the parameters θ, K of Ref. 28 as $\theta = (2\xi_{\mathrm{MF}}^2)^{-1}$, $K = (C^2/u)(1+\theta)$, where $\theta = 0$ corresponds to the displacive limit and $\Theta = \infty$ to the Ising limit]. If we interpret eq. (5) in the sense of eq. (4a) as the result of coarse-graining of a more microscopic model where lengths still are measured in units of the original lattice spacing, we have

$$\mathscr{H}_{\mathrm{GLW}} = \frac{l^d r^2}{u}\left\{\sum_i \left[\frac{-m^2(i)}{2}+\frac{m^4(i)}{4}\right] + \left(\frac{\xi_{\mathrm{MF}}}{l}\right)^2 \sum_{\langle ij\rangle} [m(i)-m(j)]^2\right\} \tag{9}$$

Thus, if one would choose $l = \xi_{\mathrm{MF}}$ [note that ξ_{MF} is finite at the true T_c due to the depression of T_c from its mean-field value to lower temperatures

due to fluctuations] $\mathcal{H}_{\mathrm{GLW}}$ would have a single parameter, $l^d r^2/u$ while in the general case there are two. In terms of a ferromagnetic Ising model eq. (1), the two relevant parameters are T/T_c and the range R of the interaction. Choosing a particular value of l, the Ising model with $\{T/T_c, R\}$ is then supposedly mapped onto eq. (9) with some parameters $\{l^d r^2/u, \xi_{\mathrm{MF}}/l\}$. Of course, there should be a simple proportionality between R and ξ_{MF} when $R \to \infty$, and since in this limit eq. (9) trivially follows from an expansion of the molecular field results for the original Ising model, we are interested mainly in the opposite limit where R is small, e.g., the case of nearest-neighbor interaction in eq. (1) only.

An equivalent rescaling of eq. (5) is obtained by rearranging the term $[\Phi(i) - \Phi(j)]^2 = \Phi^2(i) + \Phi^2(j) - 2\Phi(i)\,\Phi(j)$ which yields

$$\mathcal{H}_{\Phi^4} = \sum_i \left[\frac{r + 2dC}{2} \Phi^2(i) + \frac{u}{4} \Phi^4(i) \right] - C \sum_{\langle ij \rangle} \Phi(i)\,\Phi(j) \tag{10}$$

Choosing now [for $r + 2dC < 0$ the normalization $m(i) \equiv \Phi(i)/(-(r+2dC)/u)^{1/2}$, one finds

$$\mathcal{H}_{\Phi^4} = \tilde{\alpha} \sum_i \left[-\frac{1}{2} m^2(i) + \frac{1}{4} m^4(i) \right] - \tilde{\beta} \sum_{\langle ij \rangle} m(i)\, m(j) \tag{11a}$$

with $\tilde{\alpha} = (r + 2dC)^2/u$, $\tilde{\beta} = -C(r + 2dC)/u$. Of course, this normalization of the model is rather arbitrary, but it can be uniquely related to other choices of normalizing the model eq. (5); e.g., the parameters K and $\tilde{L}$ of Ref. 24 are related to $\tilde{\alpha}$, $\tilde{\beta}$, as $K = \tilde{\beta}(1 + 2d\tilde{\beta}/\tilde{\alpha})$, $\tilde{L} = \tilde{\alpha}(1 + 2d\tilde{\beta}/\tilde{\alpha})^2/4$ [or, vice versa, $\tilde{\alpha} = 4\tilde{L} - 4dK + (d^2K^2/\tilde{L})$, $\tilde{\beta} = K - (dK^2/2\tilde{L})$]. The advantage of the normalization eq. (11a) is that it very clearly exhibits the Ising limit; if $\tilde{\alpha} \to \infty$ the variables $m(i)$ are essentially restricted to ± 1 and one is explicitly left with the Ising model and with coupling constant $J/k_B T = \tilde{\beta}$. Thus, one can immediately infer one limiting case of the critical line $\tilde{\beta} = \tilde{\beta}_c(\tilde{\alpha})$ in the $\tilde{\alpha}$, $\tilde{\beta}$ plane where the phase transition from order to disorder occurs, namely $\lim_{\alpha \to \infty} \tilde{\beta}_c(\tilde{\alpha}) = (J/k_B T_c)_{\mathrm{Ising}}$. The critical line $\tilde{\beta}_c(\alpha)$ ends in the point $\tilde{\alpha} = \tilde{\beta} = 0$; this point is not a special limit in the normalization of eq. 8 or of Ref. 24, respectively, it simply corresponds to the choice $K = (2/d)\tilde{L}$, which leads to $\tilde{\beta}_c(\tilde{\alpha}) \approx (\tilde{\alpha} K_c/2d)^{1/2}$ for $\tilde{\alpha} \to 0$. In between these limits we expect the critical line $\tilde{\beta}_c(\tilde{\alpha})$ to increase monotonically, which is borne out by the numerical calculation (Section 4).

For $r + 2dC > 0$, on the other hand, we have to choose the normalization $m(i) \equiv \Phi(i)/(((r + 2dC)/u)^{1/2})$ to find

$$\mathcal{H}_{\Phi^4} = \tilde{\alpha} \sum \left[\frac{1}{2} m^2(i) + \frac{1}{4} m^4(i) \right] - \tilde{\beta} \sum_{\langle ij \rangle} m(i)\, m(j) \tag{11b}$$

with $\tilde{\alpha} = (r + 2dC)^2/u$, $\tilde{\beta} = C(r + 2dC)/u$, and the transformation formulas $K = -\tilde{\beta}(1 - 2d\tilde{\beta}/\tilde{\alpha})$, $\tilde{L} = \tilde{\alpha}(1 - 2d\tilde{\beta}/\tilde{\alpha})^2/4$, or $\tilde{\alpha} = 4\tilde{L} - 4dK + (d^2K^2/\tilde{L})$, $\tilde{\beta} = -K + (dK^2/2\tilde{L})$. The displacive limit occurs for $\tilde{\alpha} = 2d\tilde{\beta}$, and since the critical line ends there in a point $K_c = 0$, $\tilde{L} = 0$, this corresponds in eq. (11b) to the limit $\tilde{\alpha}, \tilde{\beta} \to \infty$ $[\tilde{\alpha}_c(\tilde{\beta})/\tilde{\beta} = 2d]$.

3. MONTE-CARLO PROCEDURES

In simulating directly a model such as eq. (11) by standard Monte-Carlo procedures,[38] one encounters the difficulty that the local variable $m(i)$ is not bounded but rather can exist in the full interval, $-\infty \leqslant m(i) \leqslant +\infty$. The obvious recipe to replace this interval by a finite one, $-a \leqslant m(i) \leqslant +a$, either gives rise to serious inaccuracies due to truncation effects (if a does not exceed unity significantly, as done in Ref. 31) or leads to a very poor convergence, particularly for large $\tilde{\alpha}$, since then most of the trial values $m(i)$ chosen would be such that the single-site probability p_i

$$p_i \propto \exp\{-\tilde{\alpha}[\mp \tfrac{1}{2}m^2(i) + \tfrac{1}{4}m^4(i)]\} \tag{12}$$

would be very small. Note that the two signs in eq. (12) correspond to the two cases of eqs. (11a), (11b). Clearly, then, it is preferable to already generate the trial values of $m(i)$ with the single-site probability eq. (12) for large $\tilde{\alpha}$. In order to do this efficiently we proceed as follows: We split the Hamiltonian eq. (11) into two parts[3]

$$\begin{aligned} \mathcal{H} &= \mathcal{H}_1 + \mathcal{H}_2, \qquad \mathcal{H}_1 = -\tilde{\beta} \sum_{\langle ij \rangle} m(i)\, m(j) \\ \mathcal{H}_2 &= \tilde{\alpha} \sum_i \left[\mp \frac{1}{2} m^2(i) + \frac{1}{4} m^4(i) \right] \end{aligned} \tag{13}$$

and transform the expression for the average of an observable $A(X)$ in the canonical ensemble (phase-space points being symbolically denoted by X)

$$\langle A \rangle = \frac{1}{Z} \int dX\, A(X) \exp[-\mathcal{H}_1(X) - \mathcal{H}_2(X)] \tag{14a}$$

$$= \int dX \exp[-\mathcal{H}_1(X) - \mathcal{H}_2(X)] \tag{14b}$$

[3] Related ideas have been used to carry out the Monte-Carlo integration step involved in the real-space renormalization group approaches of Refs. 24 and 25. An elegant alternative to the present procedure is used by Bruce.[47]

by defining a new measure $\lambda(X)$ as

$$d\lambda(X) = \frac{1}{Z''} \exp[-\mathscr{H}_2(X)]\, dX \tag{15a}$$

which yields

$$\langle A \rangle = \frac{1}{Z'} \int d\lambda(X)\, A(X) \exp[-\mathscr{H}_1(X)] \tag{15b}$$

Note that Z'' in eq. (15a) is fixed by the normalization $\int d\lambda(x) = 1$. Obviously, λ can vary between $\lambda = 0$ (for $\mathscr{H}_2 \to \infty$) and $\lambda = 1$ (for $\mathscr{H}_2 \to 0$); thus, a homogeneously distributed set of points in the phase space $(-\infty < x < +\infty)$ is mapped on the interval [0, 1] with a density governed by the factor $\exp[-\mathscr{H}_2(x)]$ by means of the cumulative distribution

$$C(y) = \int_{-\infty}^{y} d\lambda(x) \Big/ \int_{-\infty}^{+\infty} d\lambda(x)$$

$$= \int_{-\infty}^{y} \exp\left[-\tilde{\alpha}\left(\mp\frac{m^2}{2} + \frac{m^4}{4}\right)\right] dm \Big/ \int_{-\infty}^{+\infty} \exp\left[-\tilde{\alpha}\left(\mp\frac{m^2}{2} + \frac{m^4}{4}\right)\right] dm \tag{15c}$$

In practice it is convenient to restrict the integration in eq. (15c) up to a cutoff parameter $\pm y_{\max}$ instead of $\pm\infty$, which in the present calculation was chosen as $y_{\max} = [1 + (26/\tilde{\alpha})^{1/2}]^{1/2}$, which means we cut off the weight function at a value $\exp[-6.5]$. Now, dividing the interval $-y_{\max}, y_{\max}$ into n intervals with length $2y_{\max}/n$, we tabulate the values of $C(y)$ for any of these intervals. Thus, we may generate spin variables $m \in [-y_{\max}, y_{\max}]$ according to the measure eq. (15a) by just generating random numbers in the interval [0, 1]. Then, entering these values into the table, we obtain the corresponding values of the variable m. We found $n = 1000$ to provide sufficient accuracy for present purposes.

Having thus chosen a new trial value $m(i)$ for a site i from this table, the Boltzmann factor required to compute the transition probability in the standard Metropolis approach[38] involves the Ising-type Hamiltonian $\mathscr{H}_1$ [(eq. (13)] only.

For example, Fig. 1 shows the single-site probability distribution for three cases which were extensively studied, $\tilde{\alpha} = 0.333$ for the $+$sign in eq. (15c) and $\tilde{\alpha} = 0.175$ and $\tilde{\alpha} = 2.5$ [for the $-$sign in eq. (15c)]. These curves, sampled for $\tilde{\beta} = 0$, simply represent eq. (12), which is a check on the accuracy of the procedure.

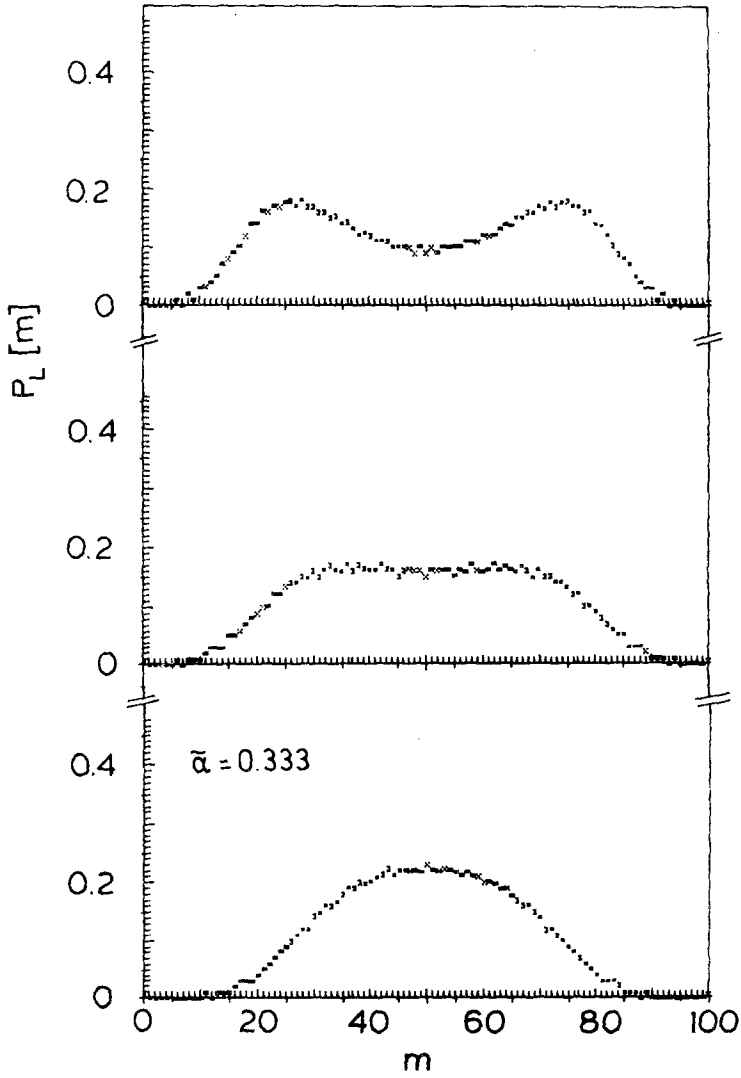

Fig. 1. Probability distribution p_i of the local spin variable $m(i)$ for $\tilde{\beta}=0$ and (a) $\tilde{\alpha}=2.5$ and (b) $\tilde{\alpha}=0.175$, as obtained from the sampling technique based on eq. (15). The interval $[-y_{\max}, +y_{\max}]$ is divided into one hundred equal subintervals for this histogram, and 1.10^6 random numbers were used to generate it. These cases refer to eq. (11a), while case (c) refers to eq. (11b) and the choice $\tilde{\alpha}=0.333$.

The quantities calculated in the present study are the order parameter $\bar{M}_L$,

$$\bar{M}_L = \langle M \rangle, \qquad M \equiv \left| \sum_i m(i) \right| \Big/ N \tag{16}$$

for a number of lattice sizes up to $N = L \times L = 60 \times 60$, and applying fully periodic boundary conditions. We also obtain the susceptibility χ_L

$$\chi_L = N[\langle M^2 \rangle - \langle M \rangle^2] \tag{17}$$

and the reduced fourth-order cumulant

$$U_L^{\text{tot}} = 1 - \frac{\langle M^4 \rangle}{3\langle M^2 \rangle^2} \tag{18}$$

While eq. (18) is a characteristic measure of the magnetization distribution of the total system, it is also interesting to compute the corresponding quantity of the local single-site magnetization probability distribution $p(m)$,

$$U^{\text{loc}} = 1 - \frac{\langle m^4 \rangle}{3\langle m^2 \rangle^2} \tag{19}$$

Note that U^{loc} can be calculated trivially from eq. (12) only for $\tilde{\beta} = 0$, where the spins $m(i)$ at different sites i are not coupled, while in the presence of the coupling $\mathscr{H}_1$ [eq. (13)] the resulting single-site magnetization distribution gets modified, as will be discussed below.

Typically the system was started in an "ordered" configuration (i.e., $m(i) = y_{\max}$ for all i) and several hundred Monte-Carlo steps per site were discarded in order to allow the system to reach equilibrium, while runs of 2.10^4 Monte-Carlo steps per site were performed for obtaining the averages, eqs. (16)–(19). Of course, in the critical region for $L \geqslant 20$, larger equilibration times are needed to obtain very precise data.

4. MONTE-CARLO RESULTS

Figure 2 shows the variation of the order parameter $\bar{M}$ with growing $\tilde{\beta}$ for three cases, namely $\tilde{\alpha} = 0.333$ for eq. (11b) [this yields a single peak in the single-site distribution, cf. Fig. 1, and hence a single minimum in the "single site potential"] and [for eq. (11a)], $\tilde{\alpha} = \tilde{\beta}$ (since $\tilde{\alpha}_c = 0.175$, this corresponds to a weakly modulated single-site potential $\mathscr{H}_2$; cf. Fig. 1) and $\tilde{\alpha} = 2.5$ (strongly modulated single-site potential). In the latter case, the local cumulant U^{loc} also is included; it is seen that U^{loc} is rather large also

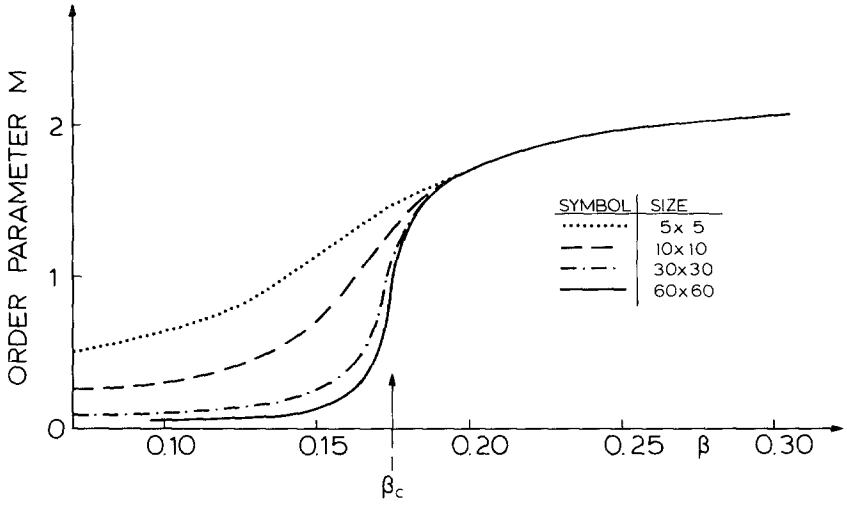

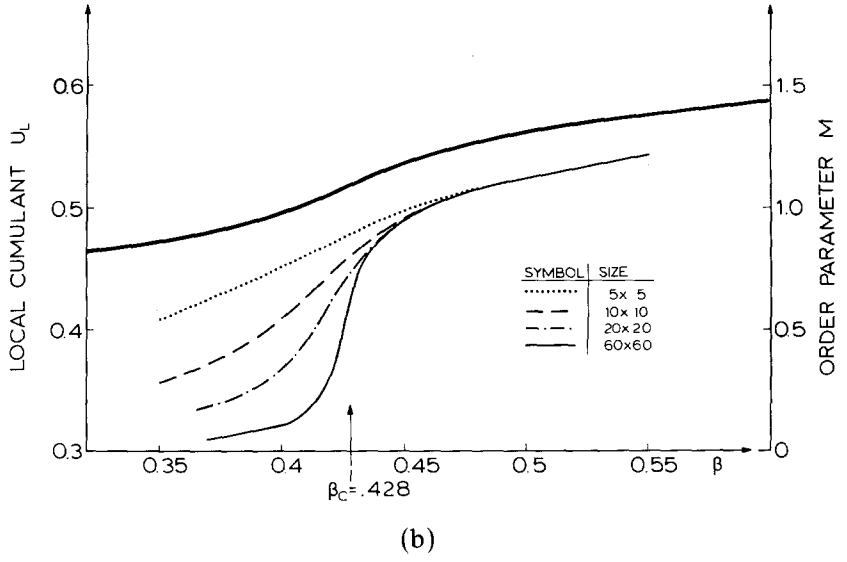

Fig. 2. Variation of the order parameter $\bar{M}_L$, eq. (16), with $\tilde{\beta}$ for the model eq. (11a), and (a) $\tilde{\alpha} = \tilde{\beta}$, (b) $\tilde{\alpha} = 2.5$, and for the model eq. (11b) for (c) $\tilde{\alpha} = 0.333$. Lattices with linear dimensins $L = 5$, 7, 10, 14, 20, 30, and 60 are shown as indicated. The thick line in (b) shows the variation of the local cumulant U^{loc} (within the thickness of this curve the various values of L coincide).

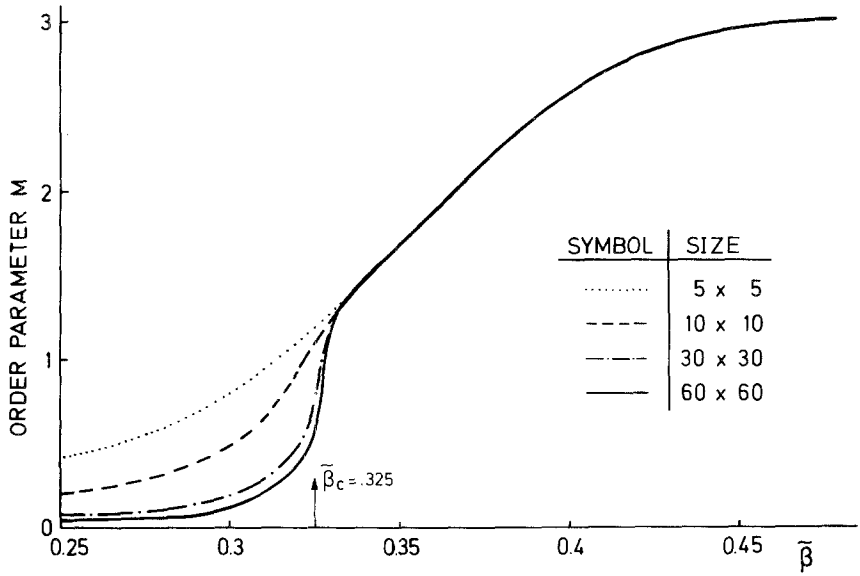

(c)

Fig. 2 (*continued*)

in the disordered regime ($\tilde{\beta} < \tilde{\beta}_c$), reflecting the pronounced order–disorder character of the transition in this case. Note that while $\bar{M}$ shows the typical finite-size "tails" in the disordered regime, U^{loc} depends on the finite total lattice sizes only very little. The values of the critical coupling $\tilde{\beta}_c$ are obtained from the cumulant intersection method[6]; see below. What is noticeable from Fig. 2 is also the different scale of the order parameter—in the case of $\tilde{\alpha} = \tilde{\beta}$ ($\tilde{\alpha}_c = 0.175$) the order parameter saturates in the ordered state at a value twice as large as for $\tilde{\alpha} = 2.5$, and in both cases this saturation value is distinctly larger than the maximum of the single-site distribution, which is at $\bar{M} = 1$. This fact already shows that for $\tilde{\alpha}_c = 0.174$ the system behaves non-Ising-like although we are still far from the "displacive limit"[20,23] which occurs for the Hamiltonian eq. (11b) and $\tilde{\alpha} \to \infty$, $\tilde{\beta} = \tilde{\alpha}/4$. Apart from this feature, both the finite-size behavior of the magnetization (Fig. 2) and the susceptibility (Fig. 3) are qualitatively similar to related data for the two-dimensional Ising model.[35] Note that for the case of eq. (11b) $\tilde{\alpha} = 0.333$, there is a broad regime of $\tilde{\beta}$ where $\bar{M}_L$ increases nearly linearly with $\tilde{\beta}$ before it saturates. This behavior reflects crossover to the displacive limit. We return to these data in Section 6 below. Our estimates for the critical point are based on the cumulants U_L^{tot} of the total magnetization eq. (18); again the qualitative behavior (Fig. 4) is similar to

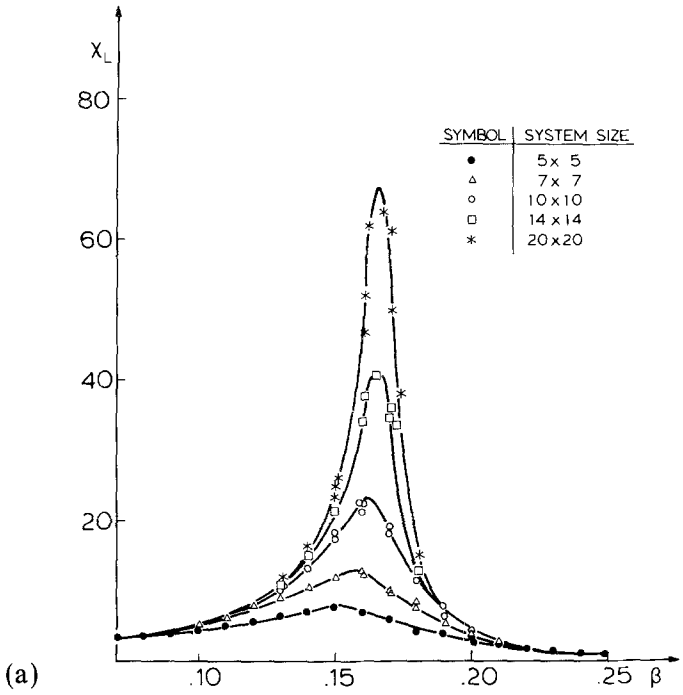
χ_L
80
60
40
20
SYMBOL | SYSTEM SIZE
5x 5
7x 7
10x10
14x14
20x20
.10
.15
.20
.25
β

(a)

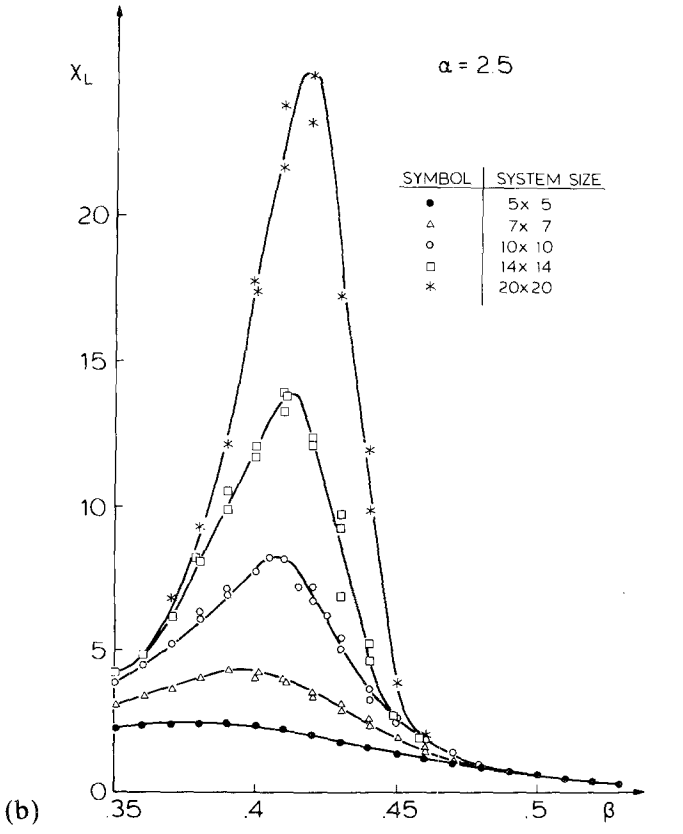
χ_L
α = 2.5
SYMBOL | SYSTEM SIZE
5x 5
7x 7
10x 10
14x 14
20x20
20
15
10
5
0
.35
.4
.45
.5
β

(b)

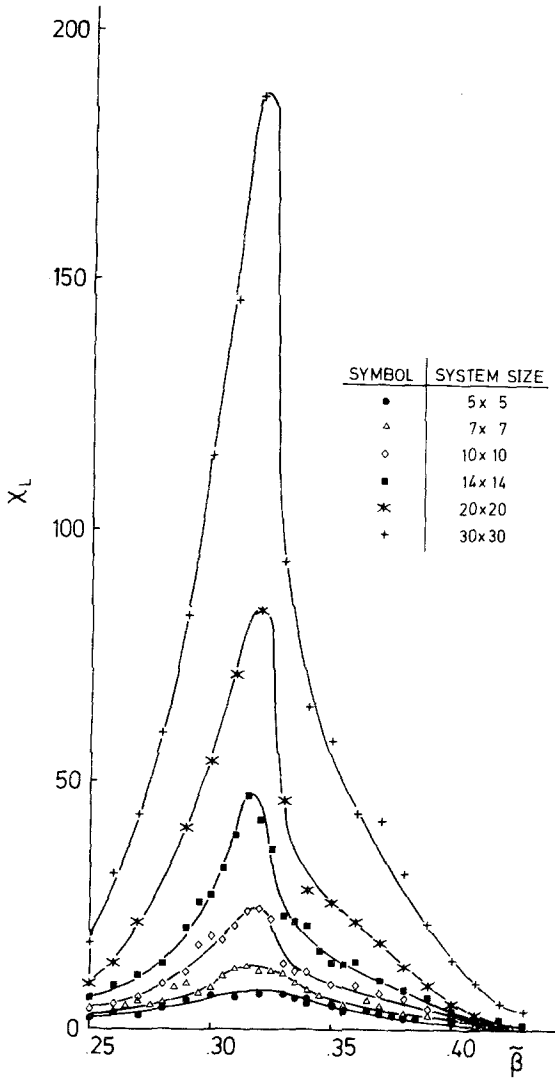

(c)

Fig. 3. Variation of the susceptibility χ_L with $\tilde{\beta}$ for the model eq. (11a) and the cases (a) $\tilde{\alpha}=\tilde{\beta}$, and (b) $\tilde{\alpha}=2.5$. Lattices of linear dimension from $L=5$ to $L=20$ are shown, as indicated in the figure. For the model eq. (11b) the case $\tilde{\alpha}=0.333$ is shown (c).

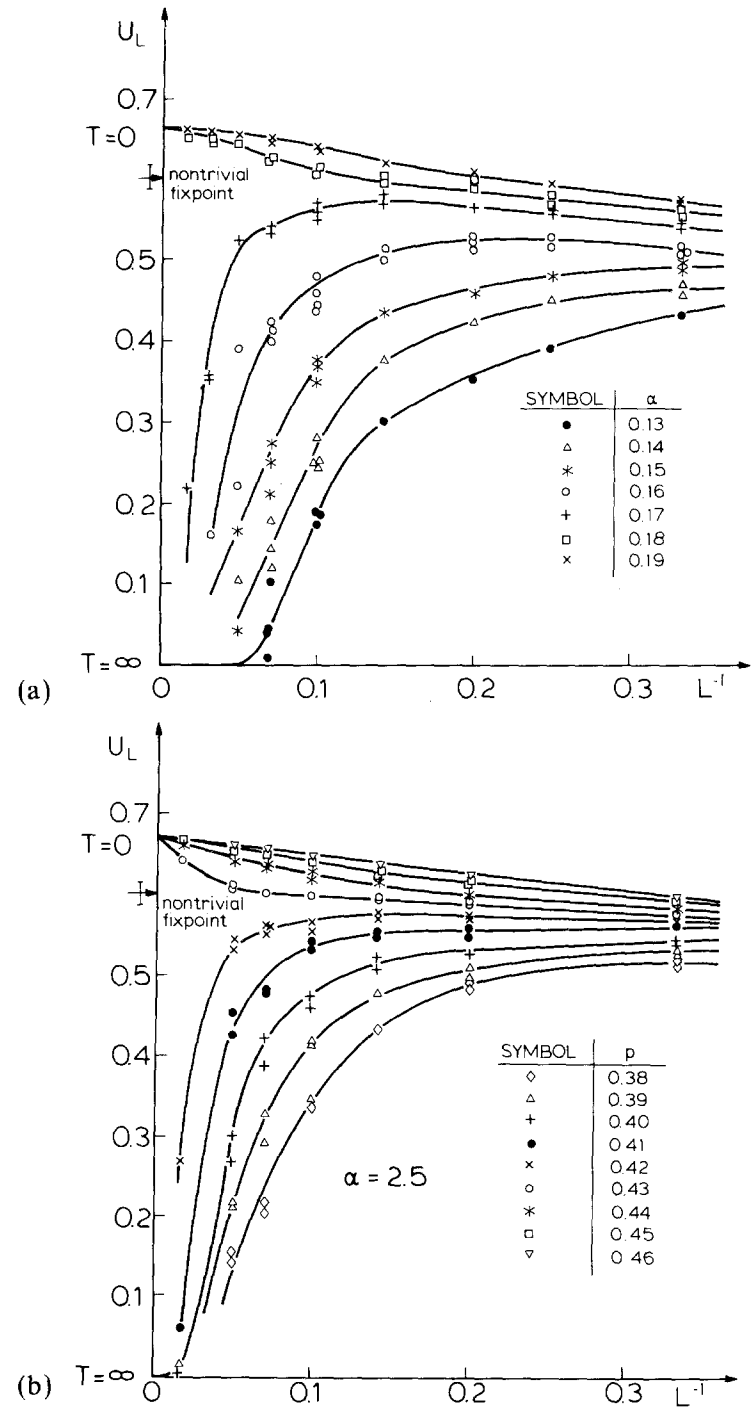

Fig. 4. Variation of the total cumulant U_L^{tot} [eq. (18)] of the magnetization-distribution function with inverse linear dimension L^{-1} for (a) $\tilde{\alpha} = \tilde{\beta}$ and (b) $\tilde{\alpha} = 2.5$, at various values of the parameter $\tilde{\beta}$. For the value U_*^{tot} at the nontrivial fixed point we obtain $U_*^{\text{tot}} \approx 0.60 \pm 0.01$ in both cases. For $\tilde{\beta} < \tilde{\beta}_c$, U_L^{tot} tends to the $T = \infty$ fixed-point value $U_*^{\text{tot}} = 0$ (single Gaussian distribution); for $\tilde{\beta} > \tilde{\beta}_c$, U_L^{tot} tends to $U_*^{\text{tot}} = \frac{2}{3}$ (double Gaussian or two-δ-function distribution).

results for the two-dimensional Ising model.[39] In addition, the data are consistent with a limiting behavior

$$\lim_{L \to \infty} U_L^{\text{tot}} \mid_{\tilde{\beta} = \tilde{\beta}_c} = U_*^{\text{tot}}$$

with a value $U_*^{\text{tot}} \cong 0.60 \pm 0.01$ which is consistent with the value $U_*^{\text{tot}} \approx 0.61$ obtained in previous Monte-Carlo work on two-dimensional Ising models[39] (and the very accurate result $U_*^{\text{tot}} \cong 0.618$ due to transfer matrix calculations.[40] This fact is gratifying, since it is an indication that the model studied indeed falls into the Ising universality class, as expected. Note that for a given universality class U_*^{tot} must take a universal value, independent of the irrelevant parameters of the Hamiltonian.[6]

In principle, the "flow diagram" Fig. 4 could be used to deduce the critical coupling $\tilde{\beta}_c$. In practice, it is convenient to plot $U_L^{\text{tot}}/U_{L'}^{\text{tot}}$ for various pairs L, L' and look at which coupling this ratio intersects unity (Fig. 5). If—and only if—all pairs (L, L') intersect in a unique point, the whole range of sizes studied belongs to the asymptotic regime $L \to \infty$, where finite-size scaling is valid and the abscissa value of this intersection point can be taken as estimate of $\tilde{\beta}_c$.[6] In practice, of course, we expect some corrections to finite-size scaling, particularly since the chosen values of L are not very large; these corrections lead to some scatter obtained in the estimates for $\tilde{\beta}_c$ from various pairs (L, L'). Figure 5 shows that this scatter is rather small for $\tilde{\alpha} = 2.5$, the case in which it is still rather close to the Ising limit because of the pronounced double-peak structure for the single-site distribution (Fig. 1). The scatter is rather pronounced for the case $\tilde{\alpha} = \tilde{\beta}$ ($\tilde{\beta}_c = 0.175$), which is further in the crossover regime between Ising and displacive behavior, as is also clear from the shallow structure of the single-site distribution.

Finally, Fig. 6(a) presents our phase diagram in the $\tilde{\alpha} - \tilde{\beta}$-plane, showing the line $\tilde{\alpha}_c(\tilde{\beta})$ separating the regime of the disordered phase from the regime of the ordered phase. We also include the value of the local cumulant, $U_{\text{crit}}^{\text{loc}}$ [eq. (19)] in this figure, for the respective critical point. Unlike U_*^{tot}, $U_{\text{crit}}^{\text{loc}}$ is not a universal quantity of the model, it varies from $U_{\text{crit}}^{\text{loc}} = \frac{2}{3}$ at the Ising limit ($\tilde{\alpha}_c \to \infty$, $\tilde{\beta}_c \cong 0.441$) to $U_{\text{crit}}^{\text{loc}} = 0$ at the displacive limit [($\tilde{\beta}_c \to \infty$, $\tilde{\alpha}_c = 4\tilde{\beta}$ in eq. (11b)]. Transformation of our data for $\tilde{\alpha}_c(\tilde{\beta})$ to the representation in terms of the variables K, $\tilde{L}$ of Ref. 24 reveals excellent agreement with the results of Burkhardt and Kinzel[24]; see Fig. 6(b). Our results on the critical line are also in agreement with the much more precise work based on the extrapolation of series expansions.[37]

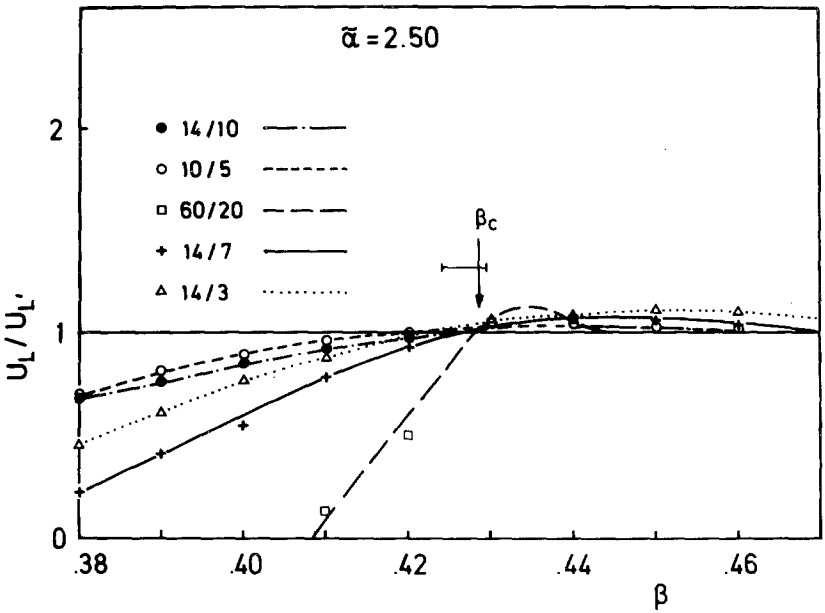

(a)

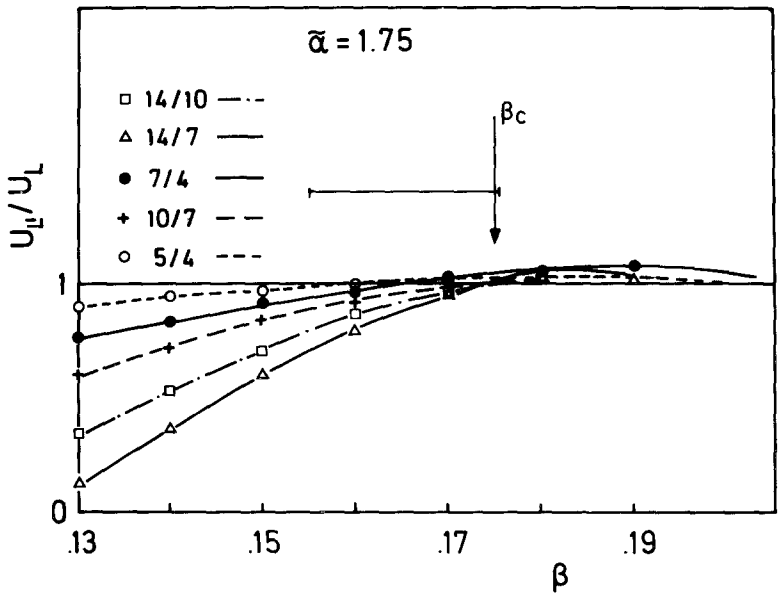

(b)

Fig. 5. Determination of the critical coupling $\tilde{\beta}_c$ from a plot of $U_L^{tot}/U_{L'}^{tot}$ versus $\tilde{\beta}$ for (a) $\tilde{\alpha} = 2.5$ and (b) $\tilde{\alpha} = \tilde{\beta}$, and various pairs (L, L').

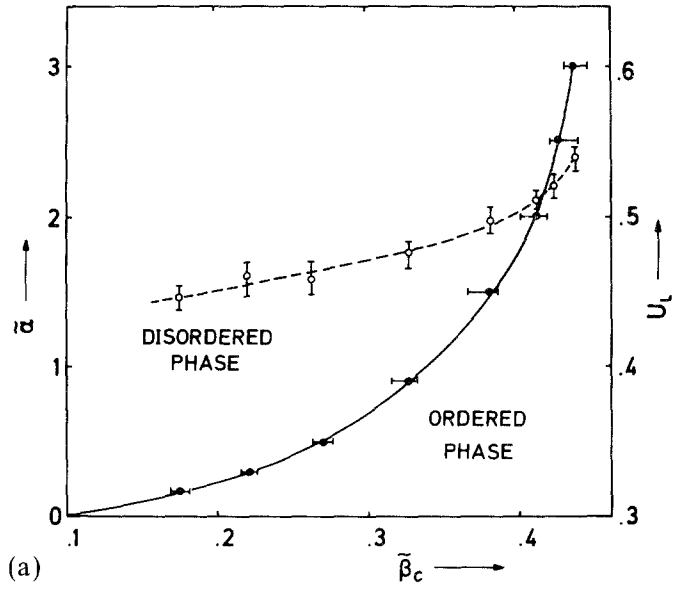

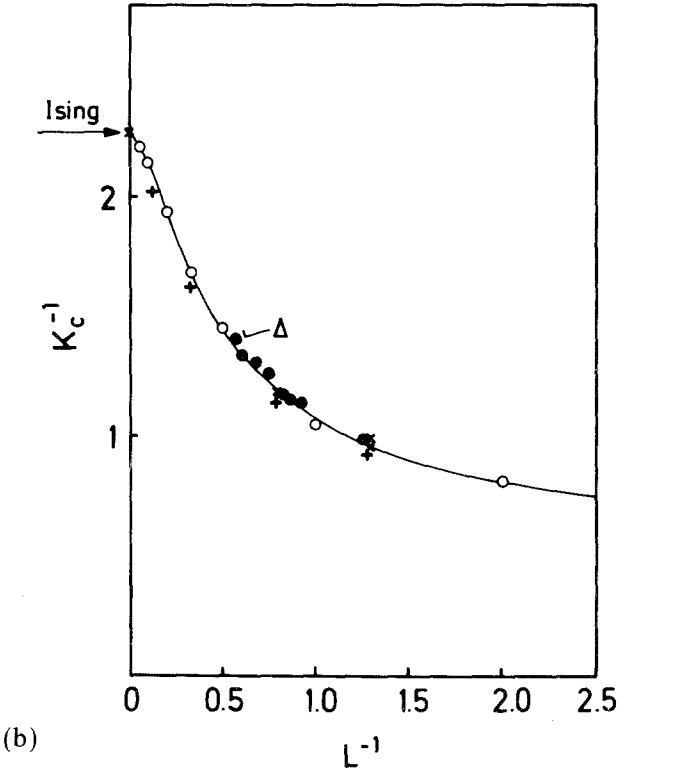

Fig. 6. (a) Dependence of the critical parameter $\tilde{\beta}$, separating the state of disorder from the ordered regimes for the model eq. (11a) at a given value of α_c (full curve). Dashed curve shows the variation of the local cumulant U^{loc}, eq. (19), at various points of the critical curve $\alpha_c = \alpha_c(\beta)$ [or $\beta_c = \beta_c(\alpha)$, respectively]. (b) Critical line expressed in terms of couplings K, $\tilde{L}$ of Ref. 24. Full dots show present calculation, open circles and standing crosses show results of Ref. 24, crosses are according to Ref. 22.

5. TEMPERATURE DEPENDENCE OF THE LOCAL-ORDER PARAMETER FLUCTUATION

Recently it has been suggested that the local density fluctuation, $\langle \rho_{\text{loc}}^2 \rangle - \langle \rho \rangle^2$, of fluids such as N_2 near their critical point can be inferred from vibrational Raman spectra, and a linear variation of $\ln[\langle \rho_{\text{loc}}^2 \rangle - \langle \rho \rangle^2]$ as a function of $(T/T_c - 1)$ was found.[32] Of course, this is consistent with the fact that the local-order parameter fluctuation stays finite at T_c; it cannot diverge at criticality while the global order parameter fluctuation does diverge [cf. eq. (17)]. In fact it is likely that the local-order parameter fluctuation is accessible for other transitions, too, by suitable experimental methods; thus, we present here Monte-Carlo results on the temperature dependence of this quantity, including unpublished previous data on Ising models at various dimensionalities.[6,41] We also a give a brief discussion of the background theory[6] on this quantity, to clarify questions which were recently raised.[33,42]

Figure 7 shows data for $\langle m^2 \rangle^{\text{loc}}$ plotted vs $\tilde{\beta}$ as obtained from the present work, as well as corresponding data for the two-dimensional Ising model. Of course, there the single-site magnetization square $S^2 \equiv 1$ is meaningless, but the quantity of interest is the mean-square magnetization $\langle \Phi^2 \rangle$ of subblocks of linear dimension l. It is seen that the shape of these curves for both models is rather similar; both $\langle m^2 \rangle^{\text{loc}}$ and $\langle \Phi^2 \rangle$ are finite at criticality and have an inflection point there. On a restricted temperature scale very close to criticality, these data may indeed look linear as well as corresponding three-dimensional data (Fig. 8).

It should be noted, however, that the temperature dependence of both $\langle m^2 \rangle^{\text{loc}}$ and $\langle \Phi^2 \rangle$ expected on theoretical grounds near T_c is not strictly linear, but rather there should be an energy-like singularity[6] which, for the Ising universality class in $d = 2$, is

$$\langle m^2 \rangle^{\text{loc}} = \langle m^2 \rangle_{T_c}^{\text{loc}} + C_1 \left(\frac{T}{T_c} - 1 \right) + C_2 \left(\frac{T}{T_c} - 1 \right) \ln \left(\frac{T}{T_c} - 1 \right) + \cdots \tag{20a}$$

where C_1, C_2 are constants while in the general case, where the specific heat exhibits a singularity proportional to $(T/T_c - 1)^{-\alpha}$ [exponent α should not be confused with the coupling parameter $\tilde{\alpha}$ in eq. (11)], one predicts

$$\langle m^2 \rangle^{\text{loc}} = \langle m^2 \rangle_{T_c}^{\text{loc}} + C_1 \left(\frac{T}{T_c} - 1 \right) + C_2 \left(\frac{T}{T_c} - 1 \right)^{1-\alpha} + \cdots T > T_c \tag{20b}$$

and analogous expressions hold for $T < T_c$. It is this energy-type singularity which is responsible for the fact that there is an inflection point of the curves in Fig. 7. Of course, since the total size of the simulated systems is

finite, there is also a finite-size rounding of the specific heat singularity in our simulations, and thus an actual divergence of the slope of the curves in Fig. 7 at T_c is not seen.

While eq. (20) also applies to a subsystem of linear dimension l of an infinite system, it does not apply to the magnetization square of a finite

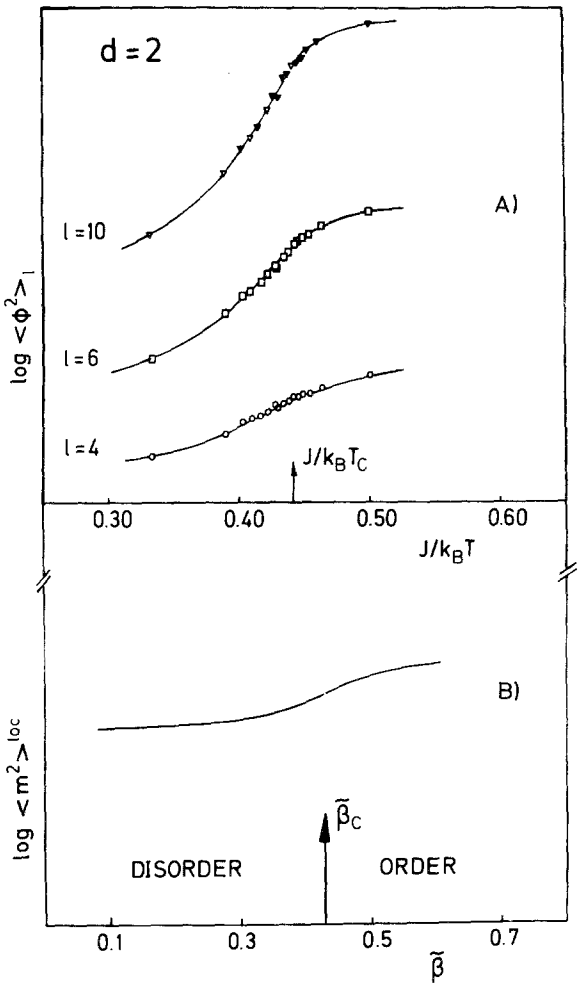

Fig. 7. Plot of $\log\langle m^2\rangle^{\mathrm{loc}}$ versus β (lower part) for the model eq. (11a) with $\tilde{\alpha} = 2.50$, and of $\log\langle \Phi^2\rangle_l$ versus $J/k_B T$ for the two-dimensional Ising square lattice for several choices of l. Arrows indicate the critical point. Ordinate scale in case (A) contains arbitrary normalization factors.

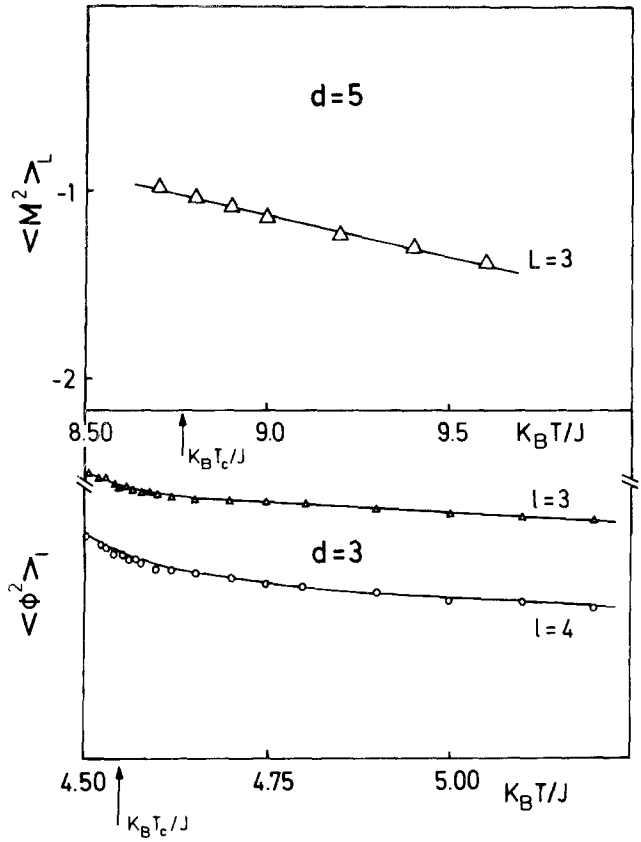

Fig. 8. Plot of $\log\langle\Phi^2\rangle_l$ versus temperature for the three-dimensional nearest neighbour Ising model and two choices of l (lower part) and of $\log\langle M^2\rangle_L$ for the five-dimensional nearest neighbour Ising model for $L=3$ (upper part). Arrows denote the critical temperatures. Ordinate scales contain arbitrary normalization factors.

system, since there occurs no singular behavior in the latter case whatsoever [C_1, C_1', C_2^+, C_3' are constants]

$$\langle\Phi^2\rangle_l = \langle\Phi^2\rangle_{l,T_c} - C_1\left(\frac{T}{T_c}-1\right) - C_2^+\left(\frac{T}{T_c}-1\right)^{1-\alpha} + \cdots \tag{21a}$$

$$\langle M^2\rangle_L = \langle M^2\rangle_{L,T_c} - C_1'\left(\frac{T}{T_c}-1\right) - C_3'\left(\frac{T}{T_c}-1\right)^2 - \cdots \tag{21b}$$

This conclusion is corroborated by the data in Fig. 8 which show a linearity over a wide temperature range in a case corresponding to eq. (21b). However, the size dependences of the terms at T_c are the same

$$\langle\Phi^2\rangle_{l,T_c} \propto l^{-2\beta/\nu}, \qquad \langle M^2\rangle_L \propto L^{-2\beta/\nu} \tag{22}$$

where β denotes the order-parameter exponent and ν the correlation length exponent, and we assume the validity of hyperscaling ($d\nu = \gamma + 2\beta$, γ being the susceptibility exponent). Equation (22) then implies that the maximum value of the susceptibility $\chi_L^{\max}$, cf. eq. (17) with $N = L^d$, scales as $\chi_L^{\max} \propto L^{\gamma/\nu}$. [In the mean-field limit, however, hyperscaling is invalid, and one rather has $\chi_L^{\max} \propto V^{1/2} = L^{d/2}$.[43]] While in the subsystem geometry the maximum slope of $\langle \Phi^2 \rangle_l$ occurs precisely at the T_c of the infinite system [and is infinite there if $\alpha \geqslant 0$], the maximum slope of $\langle M^2 \rangle_L$ in general occurs at a shifted $T_c(L)$. Similarly, the quantity $\langle M^2 \rangle_L - \langle |M| \rangle_L^2$ has a rounded maximum at $T_c(L)$, while the analogous reduced fluctuation $\langle \Phi^2 \rangle_l - \langle |\Phi| \rangle_l^2$ has a true cusp at T_c, since $\langle |\Phi| \rangle_l = B(1 - T/T_c)^\beta$ independent of l, while $\langle |M| \rangle_L$ does not vanish at $T_c(L)$ or $T_c(\infty)$, respectively, and is also a smooth nonsingular function of temperature. Thus, for $T < T_c$, eq. (21) is replaced by

$$\langle \Phi^2 \rangle_l - \langle |\Phi| \rangle_l^2 = \langle \Phi^2 \rangle_{l,T_c} - C_1 \left(\frac{T}{T_c} - 1 \right) + C_2^- \left(1 - \frac{T}{T_c} \right)^{1-\alpha} - B^2 \left(1 - \frac{T}{T_c} \right)^{2\beta} + \cdots \tag{23a}$$

$$\langle M^2 \rangle_L - \langle |M| \rangle_L^2 = \langle M^2 \rangle_{L,T_c} - C_1'' \left(\frac{T}{T_c} - 1 \right) - C_3'' \left(\frac{T}{T_c} - 1 \right)^2 - \cdots \tag{23b}$$

Note that eq. (23b) holds for both $T > T_c$ and $T < T_c$ and has the same form as eq. (21b).

6. FINITE-SIZE SCALING

The finite-size scaling hypothesis[34] implies that the finite-system magnetization $\bar{M}_L$ and susceptibility χ_L can be scaled as functions of the linear dimension L and the reduced coupling $t = 1 - \tilde{\beta}_c/\tilde{\beta}$, as follows

$$\bar{M}_L L^{\beta/\nu} = \tilde{M}(tL^{1/\nu}), \qquad t \to 0, \quad L \to \infty \tag{24a}$$

$$\chi_L L^{-\gamma/\nu} = \tilde{\chi}(tL^{1/\nu}), \qquad t \to 0, \quad L \to \infty \tag{24b}$$

where β, γ, ν are the critical exponents and $\tilde{M}$, $\tilde{\chi}$ the respective scaling functions. Indeed eq. (24) works nicely already for $L = 5$ to $L = 60$, the range considered here, for the $d = 2$ Ising model[35]; there, corrections to finite-size scaling are so small that even rather small systems are already rather close to the asymptotic limit considered in eq. (24).

Figures 9–13 show that this is no longer true for the model eq. (11), particularly if one moves closer toward the displacive limit. As concluded

previously,[22,24] we do expect that the exponents along the whole critical line $\tilde{\beta} = \tilde{\beta}_c(\tilde{\alpha})$ should retain the Ising values, $\beta = 1/8$, $\gamma = 7/4$, $\nu = 1.0$ in our case,[15] apart from the displacive limit, where the exponents should jump discontinuously to their mean-field values $\beta = \nu = \frac{1}{2}$, $\gamma = 1$. Since we have determined $\tilde{\beta}_c(\tilde{\alpha})$ independently from the cumulant analysis, Fig. 5, there is

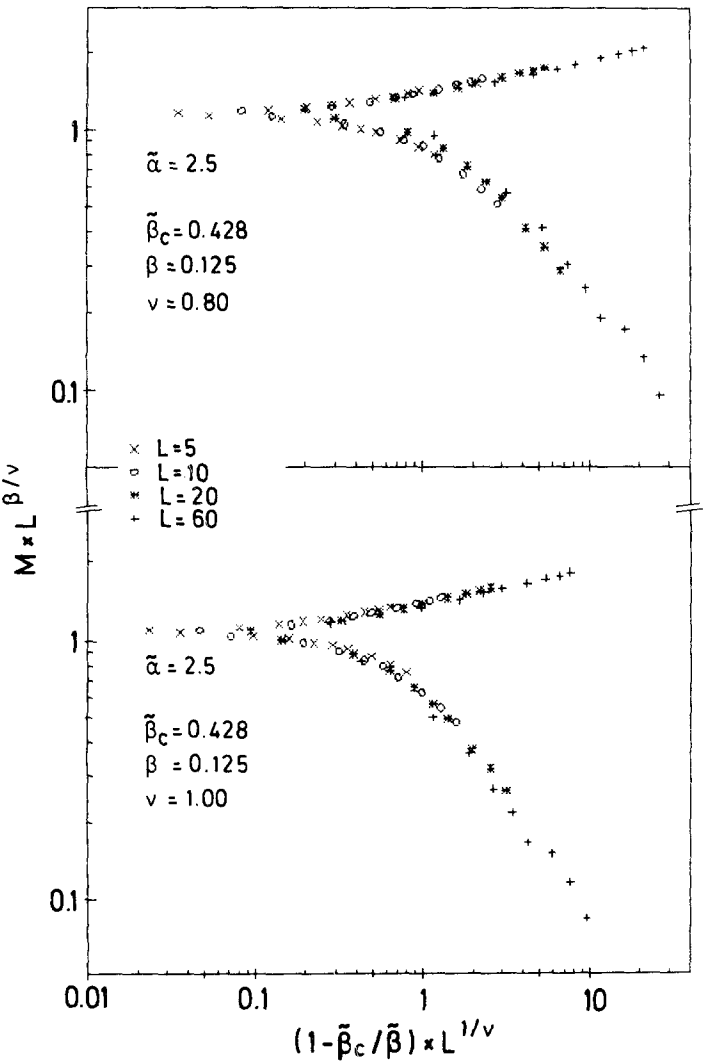

Fig. 9. Plot of $\bar{M}_L L^{\beta/\nu}$ versus $tL^{1/\nu}$ for the case $\tilde{\alpha} = 2.5$, $\tilde{\beta}_c = 0.428$, [model eq. (11a)] and $L = 5$, 10, 20, 60, as indicated, for the choice of Ising exponents (a) $\beta = 0.125$, $\nu = 1.0$ and (b) $\beta = 0.125$, $\nu = 0.8$.

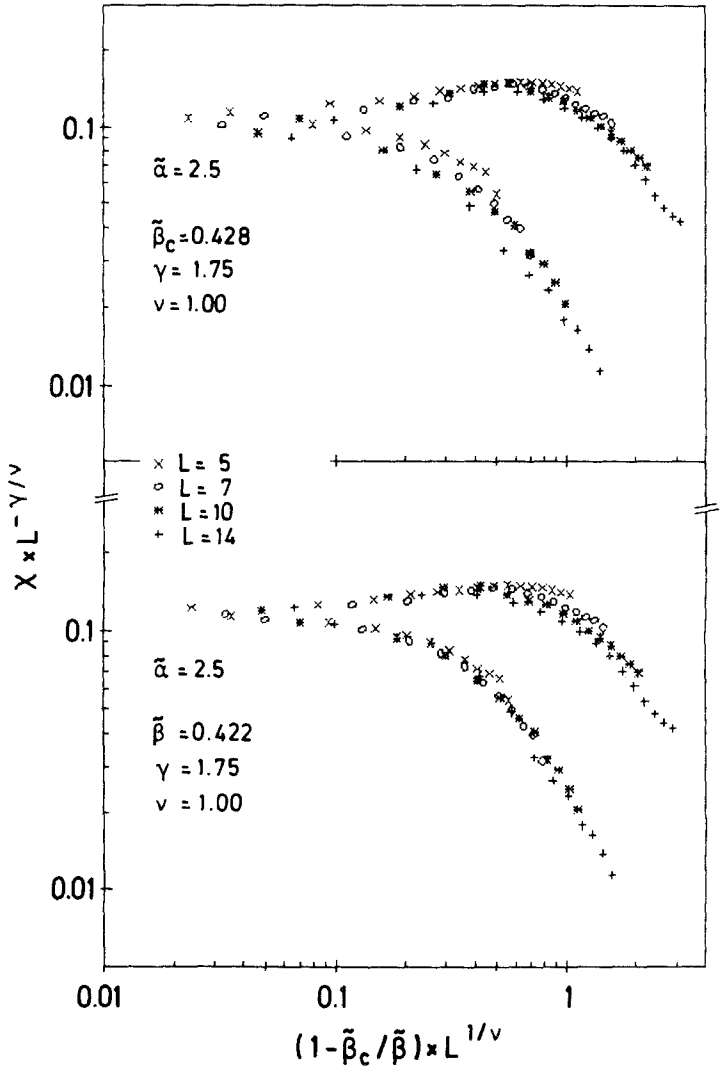

Fig. 10. Plot of $\chi_L L^{-\gamma/\nu}$ versus $tL^{1/\nu}$ for the case (a) $\tilde{\alpha}=2.5$, $\tilde{\beta}_c=0.428$ or (b) $\tilde{\beta}_c=0.422$ and $L=5$, 7, 10, 14, as indicated, choosing Ising exponents $\beta=0.125$ and $\gamma=1.75$ for both assumptions on the precise value of the critical coupling $\tilde{\beta}_c$. These data show that the uncertainty in $\tilde{\beta}_c$ does not influence our finite-size analysis significantly, for the accessible range of L and t.

no adjustable parameter in eq. (24) and the family of curves shown in Fig. 2 (or Fig. 3) should collapse in the representation of eq. (24) on a single curve, the scaling function. This "data collapsing" still works rather well for the case $\tilde{\alpha} = 2.5$, $\tilde{\beta}_c = 0.428$ (Figs. 9a, 10a) and the scatter of the points is not significantly improved by choosing other values of the

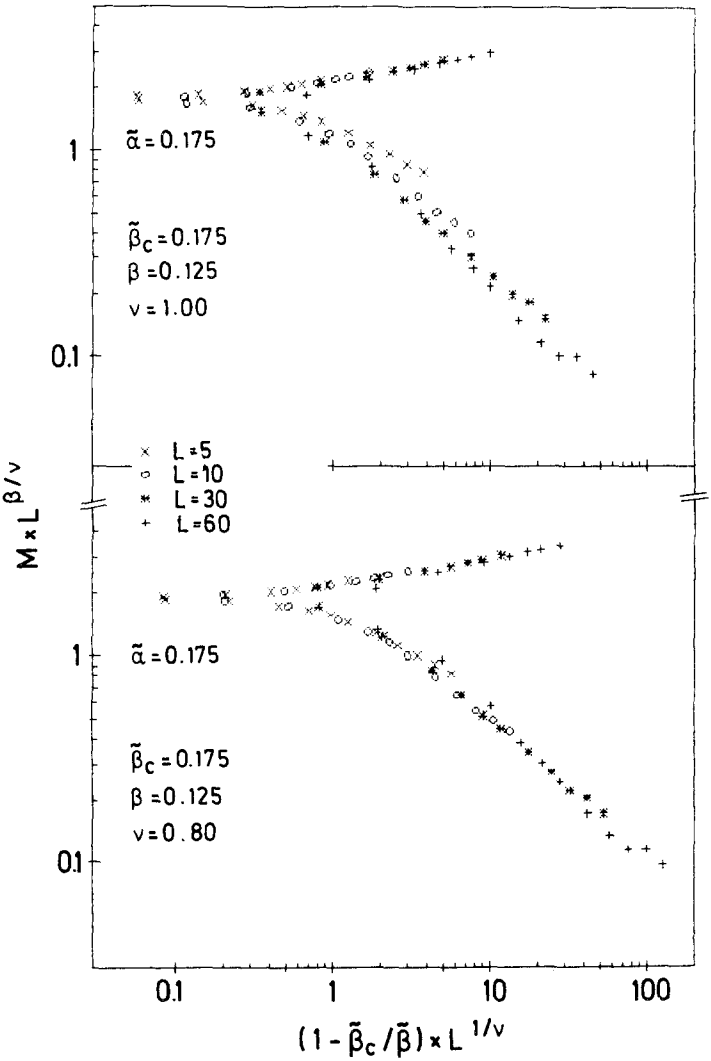

Fig. 11. Plot of $\bar{M}_L L^{\beta/\nu}$ versus $tL^{1/\nu}$ for the case $\tilde{\alpha} = \tilde{\beta}$ ($\tilde{\beta}_c = 0.175$, for the model eq. (11a) and $L = 5$, 10, 30, 60, as indicated, for the choice of Ising exponents (a) $\beta = 0.125$, $\nu = 1.0$ and (b) $\beta = 0.125$, $\nu = 0.80$.

exponents (see, e.g., Figs. 9b, 10b). But there is dramatic scatter for the cases closer to the displacive limit. For example, Figs. 11(a), 12(a) show the data for $\tilde{\alpha} = \tilde{\beta}$ ($\tilde{\beta}_c = 0.175$); in this case a significantly better fit would be obtained if we choose a significantly lower value of ν, $\nu \approx 0.8$ (Figs. 11b, 12b). However, we think that this observation just reflects that we have entered the crossover regime toward the displacive limit: in this crossover regime the asymptotic exponents are still the Ising ones, but one must get

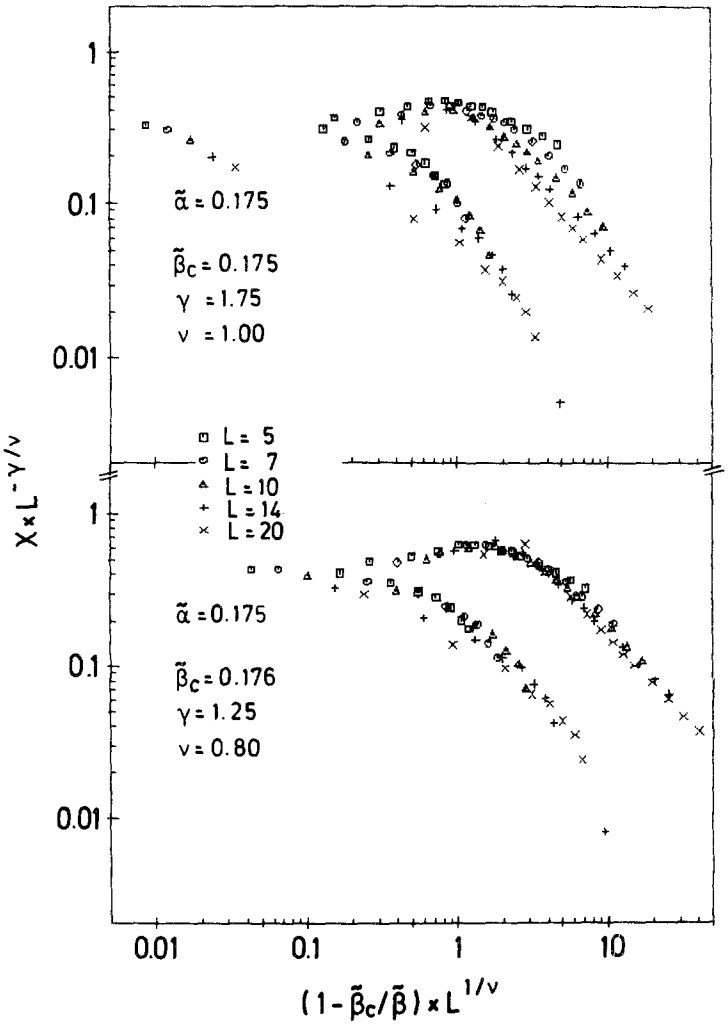

Fig. 12. Plot of $\chi_L \cdot L^{-\gamma/\nu}$ versus $t \cdot L^{1/\nu}$ for the case $\tilde{\alpha} = \tilde{\beta}$ ($\tilde{\beta}_c = 0.175$) and $L = 5, 7, 10, 14, 20$, as indicated in the figure, choosing Ising exponents (a) $\beta = 0.125$, $\gamma = 1.75$ and (b) $\gamma = 1.25$, $\nu = 0.080$.

closer and closer to criticality the closer one gets to the displacive limit in order to reach the asymptotic critical region. In fact, the scatter of estimates for $\tilde{\beta}_c$ obtained from the cumulant intersections (Fig. 5b) *proves* that the sizes used here are *not* in the asymptotic region where finite-size scaling holds, in the present case. Therefore, the apparently good fit seen in Figs. 11(b), 12(b) is somewhat meaningless; at best, $\nu \approx 0.8$ can be interpreted as an "effective exponent" seen in some intermediate regime in the

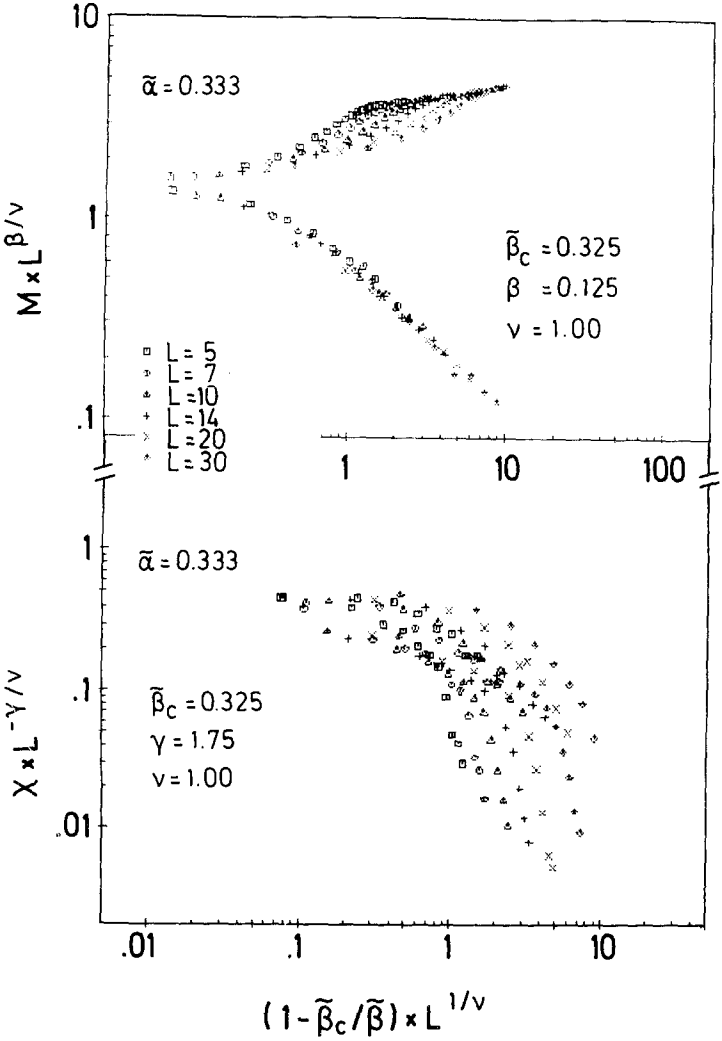

Fig. 13. Plot of (a) $\bar{M}_L L^{\beta/\nu}$ and of (b) $\chi_L L^{-\gamma/\nu}$ versus $tL^{1/\nu}$ for the case $\tilde{\beta} = 0.333$, $\tilde{\beta}_c = 0.325$ [model eq. (11b)] for various lattice sizes as indicated, and Ising exponents $\beta = 0.125$, $\gamma = 1$.

crossover region. In no case could the claim of $\gamma \approx 2$ of Ref. 18 for the continuous spin Ising model explain our data, which imply an effective exponent of $\gamma \approx 1.2$ to 1.4 (Fig. 12b).

The straight lines to which the scaling functions $\tilde{M}(x)$, $\tilde{\chi}(x)$ tend for large x can be represented by the following power laws (for the coupling $\tilde{\alpha} = 2.5$)

$$\tilde{M}(x) \cong 1.3x^{0.125}, \qquad \tilde{\chi}(x) \cong 0.023x^{-1.75}, \qquad \tilde{\beta} > \tilde{\beta}_c \tag{25a}$$

$$\tilde{M}(x) \cong 0.6x^{-0.875}, \qquad \tilde{\chi}(x) \cong 1.50x^{-1.75}, \qquad \tilde{\beta} > \tilde{\beta}_c \tag{25b}$$

Here we have chosen for the exponents the values theoretically expected for the Ising model in order to be able to estimate roughly the critical amplitudes B, C^+, C^- in the relations $\bar{M}_\infty = Bt^\beta$, $\chi_\infty^+ = C^+(-t)^{-\gamma}$, $\chi_\infty^- t^{-\gamma}$ as $B \approx 1.3$, $C^+ \approx 1.50$, $C^- \cong 0.023$; the amplitude ratio $C^+/C^- \approx 65$ within our rather large errors is consistent with the value $C^+/C^- = 37.7$ known for the $d = 2$ Ising model.[44] Note that the first relation in eq. (25b) follows from putting $\bar{M}_L \propto (M^2)^{1/2} = (\chi_L/L^d)^{1/2} \propto (-t)^{\gamma/2}$. As a further inconsistency of the scaling plot involving effective exponents, Fig. 11(b), we note that the analogous relations for $\tilde{M}(x)$ would read $\tilde{M}(x) = 2.1x^{0.22}$ $(t > 0)$ and $\tilde{M}(x) = 2.6x^{-1.19}$; i.e., imply exponents β, γ distinctly different from those used to scale the data.

7. IMPLICATIONS ABOUT COARSE-GRAINING OF THE ISING MODEL

For the theory of spinodal decomposition[3,4,10] one is less interested in critical phenomena but rather wishes to use a coarse-grained Hamiltonian where the coarse-graining length l is no longer small in comparison to the correlation length ξ. While near a nonmeanfield critical point one expects the resulting coarse-grained Hamiltonian to be more complicated than eq. (9),[5] eq. (9) is appropriate in a mean-field critical region (which occurs for medium range of the forces not too close to the critical point, for polymer mixtures etc.; see e.g., Ref. 45). Then it is appropriate to use eq. (9) and identify ξ with ξ_{MF}, which implies in the normalization of eq. (11) that $\tilde{\alpha}$ and $\tilde{\beta}$ are comparable [$\tilde{\alpha} = \tilde{\beta}$ is reached for $(\xi_{MF}/l)^2 = 1/(2(2d+1))$]. This was a motivation to study the model with $\tilde{\alpha} = \tilde{\beta}$ more closely, as discussed in the previous section.

However, in the theory of spinodal decomposition, one not only uses eq. (9) but also often (Ref. 4) makes the further assumption that the reduced distribution function $p_l(\Phi_l)$ can be approximated as a sum of two Gaussians. Figure 14 shows that this double-Gaussian approximation is fairly reasonable in the regime of the ordered phase, but becomes increasingly inaccurate as the critical point is approached.

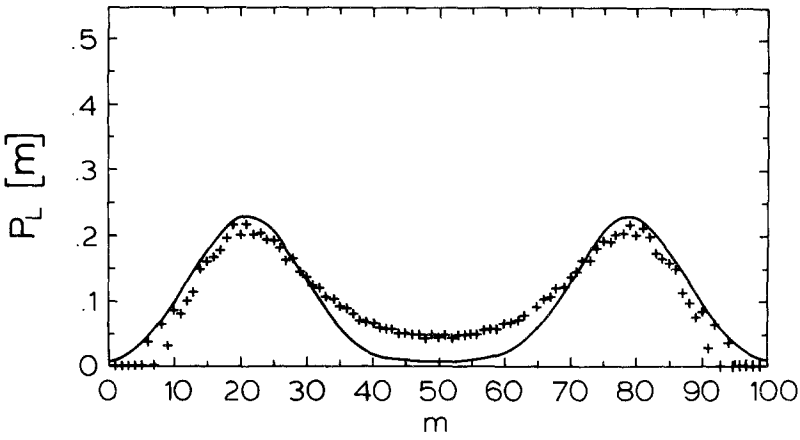

Fig. 14. Plot of the reduced single-site distribution function $P(m)$ for the model eq. (11a) for the choice (a) $\tilde{\alpha}=2.5$ and (b) $\tilde{\beta}=0.44$. Full curves show the double-Gaussian approximation.

We now return to the problem of establishing an explicit relation between the microscopic Ising Hamiltonian eq. (1) and the associated coarse-grained Hamiltonian eq. (4a). Assuming that $\mathscr{H}_{\mathrm{GLW}}$ in eq. (4a) can be taken of the simple form of eq. (5), with higher-order terms omitted, we ask: Which choice of parameters r, u, and C in eq. (5)—or $\tilde{\alpha}$ and $\tilde{\beta}$ in the rescaled version—corresponds best to eq. (1) for a reasonable choice of the coarse-graining length (e.g., $l=5$, 10, or 15, etc.)? Using both the data of Ref. 6 where $p_l(\Phi_l)$ was investigated, and the present work where $p(m)$ for eq. (11) is calculated, we can give a (preliminary) answer to this question by choosing the parameters such that a reasonable matching of $p_l(\Phi_l)$ and $p(m)$ is obtained (*for the entire critical region of both models*). The extent to which such a matching can work is nontrivial, since it is not so clear to which extent eq. (5) is a good approximation to the full $\mathscr{H}_{\mathrm{GLW}}$.

At this point one should not confuse $\mathscr{H}_{\mathrm{GLW}}$ with the fixed-point Hamiltonian $\mathscr{H}^*$ which is obtained after infinite iterations of the renormalization group transformation by which short-wave length fluctuations (starting on the length scale l) are successively integrated out: in $\mathscr{H}^*$ irrelevant higher-order terms have died out while there still should be such terms allowed for in $\mathscr{H}_{\mathrm{GLW}}$. However, since the accuracy of the present study does not warrant the attempt to fit too many parameters, we have not included any such higher-order terms in our study.

In order to check this matching of the two models in practice, we proceed as follows: First of all, the Ising criticality (J/k_BT_c) must correspond to a point on the critical line $\tilde{\beta}=\tilde{\beta}_c(\tilde{\alpha})$, but this does not specify which point. This point is specified, however, if we request $p_l(\Phi_l)_{T=T_c}$ and

$p(m)_{\tilde{\beta}=\tilde{\beta}_c}$ to be equivalent. Since for $l=5$ to 15 the local cumulant $U_l^{\text{local}} = 1-\langle \Phi_l^4\rangle_{T_C}/3\langle \Phi_l^2\rangle_{T_c}^2 \approx U_*^{\text{loc}} \approx 0{,}52$,[6] we must require $\tilde{\alpha}\approx 2.50$ since a plot of U^{loc} [eq. (19)] versus $\tilde{\alpha}$ along the critical line shows (Fig. 6a).

The next question concerns the relation of the temperature scale of T_c to the scale of $(1-\tilde{\beta}/\tilde{\beta}_c)$ occurring in our model. This question can be answered, for instance, from requesting that the temperature dependence of U_l^{local} in the Ising model matches that of U^{local} for the Φ^4 model with $\tilde{\alpha}=2.50$, i.e.

$$U_l^{\text{local}}(T)\,|_{\text{Ising model}} \equiv U^{\text{local}}(\tilde{\beta})\,|_{\phi^4\text{ model}} \tag{26}$$

The resulting mapping of the temperature scale on the scale of the parameter $\tilde{\beta}$ is presented in Fig. 15. It is seen that a rather substantial variation of the coouppling constant $\tilde{\beta}$ corresponds to a rather small variation of T/T_c only.

Using now the relation $T(\tilde{\beta})$ between the scales of T and $\tilde{\beta}$ established in Fig. 15, we can use the data for $\langle \Phi^2\rangle_l$ and $\langle m^2\rangle^{\text{loc}}$ as shown in Fig. 7 to infer the temperature dependence of the combination of parameters involved in the normalization of eq. (10) to eq. (11a), i.e.

$$\langle \Phi^2\rangle_l\,|_{T(\tilde{\beta})}/\langle m^2\rangle^{\text{loc}}\,|_{\tilde{\beta}} = [-(r+2dC)/u] \tag{27}$$

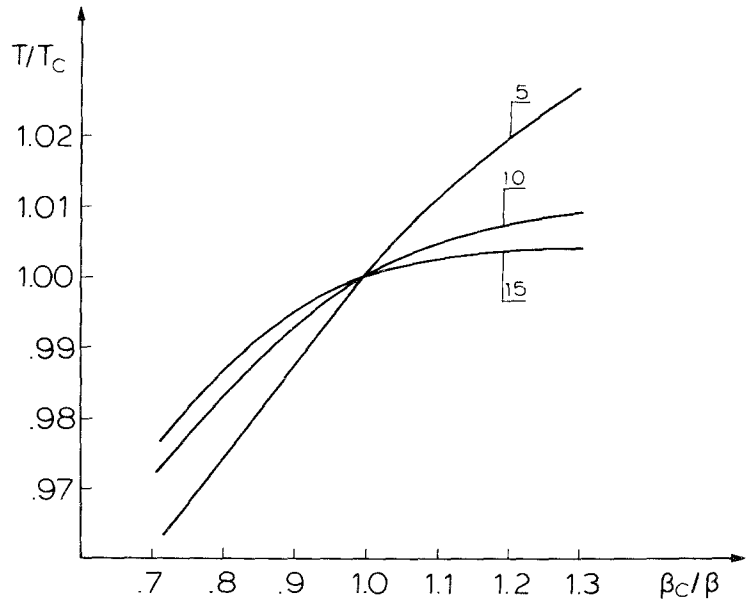

Fig. 15. Relationship between the temperature variable in the Ising model and the Φ^4 model for three choices of coarse-graining length l ($l=5$, 10, 15) as derived from eq. (26).

This is shown in Fig. 16(a) for the three values of l used in Fig. 15. It is seen that eq. (27) again yields a smooth function of temperature, as required because the parameters of the coarse-grained Hamiltonian must be nonsingular. Since $\tilde{\beta} = -C(r + 2dC)/u$, division of the function $\tilde{\beta} = \tilde{\beta}(T)$ (Fig. 15) with eq. (27) yields the temperature dependence of the constant C. This is shown in Fig. 16(b). As it should be, C depends only weakly on temperature. Using now the relation $(C/\tilde{\beta})^2 \tilde{\alpha} = u$ we also obtain the constant u, and from $\tilde{\beta}(T)$, C, r, u we straightforwardly derive $r(T)$. Remembering that eq. (5) is related to eq. (4a) by a rescaling of the lattice by a factor l, we conclude $r_l(T) = l^{-d} r(T)$, $u_l = l^{-d} u$, and $C_l = l^{2-d} C$. In this way the parameters of the free-energy functional can be obtained explicitly.

Unfortunately, the accuracy of the presently used Monte-Carlo results is too limited to take the numbers that would follow from Figs. 15 and 16

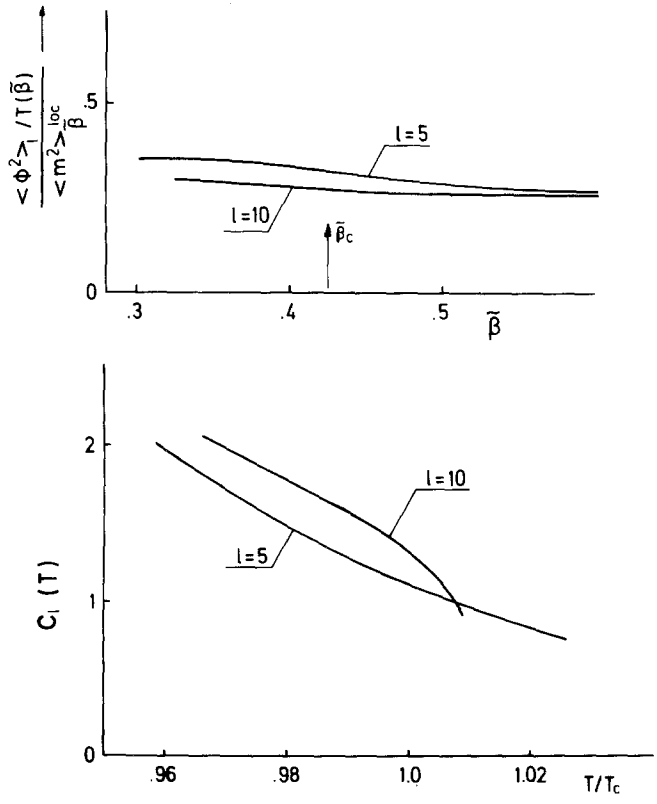

Fig. 16. (a) Plot of the ratio $\langle \Phi^2 \rangle_l / \langle m^2 \rangle^{loc}$, where $\langle \Phi^2 \rangle_l$ is chosen at a temperature $T(\tilde{\beta})$ corresponding to $\tilde{\beta}$ according to eq. (14), versus $\tilde{\beta}$ for two choices of l. (b) Plot of the coefficient $C_l(T)$ versus T for two choices of l.

very seriously. For example, for $l=5$ we would obtain $u(T_c)\approx 16.5$, $r(T_c)\approx -67.1$ while for $l=10$ we would obtain $u(T_c)\approx 23$, $r(T_c)\approx -80.1$. The lack of complete self-consistency of these numbers is recognized by considering the prediction for the magnetization of the original Ising model that would follow from Figs. 15 and 16 and the estimate for the amplitude B obtained in eq. (25a): Since near T_c from Yang's *exact* solution[46]

$$\langle S_K\rangle = \hat{B}(1-T/T_c)^{1/8}, \qquad \hat{B}\approx 1.22 \tag{28}$$

while from eqs. (2), (10), and (11)

$$\begin{aligned}\langle S_K\rangle &= \langle \Phi_l(i)\rangle = \langle m(i)\rangle [-(r+2dC)/u]^{1/2} \\ &= B[1-(\tilde{\beta}_c/\tilde{\beta})]^{1/8}[-(r+2dC)/u]^{1/2}\end{aligned} \tag{29}$$

Thus, we see that $\hat{B}=B[-(r+2dC)/u]^{1/2}[(dT/d\tilde{\beta})_{T_c}]^{1/8}$ if the Ising model and the Φ^4 model would match precisely. But from Figs. 15 and 16 we obtain for $l=5$ $(dT/d\tilde{\beta})_{T_c}\approx 0.134$, $-(r+2dC)/u\approx 3.8$, and hence $\hat{B}\approx 1.97$, while for $l=10$ $(dT/d\tilde{\beta})_{T_c}\approx 0.053$, $-(r+2dC)/u\approx 3.3$, and hence $\hat{B}\approx 1.64$. Thus, the two estimates do not exactly agree with each other, although they should because long-wavelength properties must be independent of the choice of the coarse-graining length. Moreover, neither of the estimates agree with the exact answer eq. (28).

Of course, this difficulty is not unexpected: there is considerable uncertainty in our identification of the critical parameters $\tilde{\alpha}$, $\tilde{\beta}_c$ from matching the local cumulant U^{loc} [eq. (19)] to the corresponding (not very accurate!) Ising data,[6] since U^{loc} depends on $\tilde{\beta}_c$ only weakly (Fig. 6a), and a small error in U^{loc} would introduce a large error in $\tilde{\beta}_c$. This in turn will affect the relation between T and $\tilde{\beta}$ (Fig. 15) distinctly; in addition, the latter relation will be affected by higher-order terms (Φ^6, etc.) in the coarse-grained Hamiltonian of the Ising model that surely are present in reality, but have not been included in our study.

8. CONCLUSIONS

In this paper we have undertaken a study of the Φ^4 model on a square lattice, varying a parameter by which the model interpolates between the Ising limit and the displacive limit. A Monte-Carlo algorithm was used, where one draws the single-site variable $\Phi(i)$ according to the single-site probability distribution so that standard techniques for the analysis of Monte-Carlo data could be applied. The techniques used include the cumulant intersection method, by which we located the line of critical points for the model, and finite-size scaling of order parameter and suscep-

tibility. Both techniques show pronounced difficulties, which we interpret as being due to the crossover from $2d$-Ising to mean-field behavior. Thus, while our lattice sizes are sufficient to locate the critical line in close agreement with previous work using other techniques, substantially larger lattice sizes *and* better statistics will be required for any definitive statements on critical exponents and amplitudes of the model. We have not attempted to do this since, because of the continuum nature of the variable $\Phi(i)$, techniques to speed up the program such as multispin coding[38] are not known, and even for currently available fast-vector computers very large amounts of computing time for this problem would be required.

After this study had been completed, we learned of a recent study of Bruce[47] where by extensive computations on the DAP the Ising critical behavior has been verified for the model with $r = -4C$, the "border model" of Baker.[18] Although this model is not yet close to the displacive limit, the results of Ref. 47 and ours indicate that crossover effects limit its critical region.

We have instead used our data for a preliminary feasibility check of the matching between the Φ^4 model and the coarse-grained Hamiltonian of the Ising model. The explicit form of the latter hitherto has not been known; in the present work a procedure has been illustrated by which the parameters of the Ginzburg–Landau–Wilson functional can be systematically determined, and rough estimates for the parameters involved in the leading terms have been obtained.

It clearly would be interesting to study this problem further by performing high-precision simulations of medium-range Ising models, as well as of the present Φ^4 model and the full mapping between both families of models, including also higher-order terms; there should be a one-to-one correspondence between their critical lines. It also would be very interesting to study Ising models with super-antiferromagnetic order, since their Ginzburg–Landau–Wilson Hamiltonian should be of XY-type with cubic anisotropy.

ACKNOWLEDGMENTS

One of us (A.M.) thanks the Alexander-von-Humboldt foundation for a fellowship and other support. We are also grateful to T. W. Burkhardt for a useful discussion, and to A. D. Bruce and M. E. Fisher for helpful comments.

REFERENCES

1. L. P. Kadanoff, *Physics* **2**:263 (1966).
2. K. G. Wilson, *Phys. Rev. B* **4**:3174 (1971); *Rev. Mod. Phys.* **55**:583 (1983).
3. J. S. Langer, *Ann. Phys.* **65**:53 (1971); *Physica* **73**:61 (1974).
4. J. S. Langer, M. Baron, and H. D. Miller, *Phys. Rev. A* **11**:1417 (1975); C. Billotet and K. Binder, *Z. Phys. B* **32**:195 (1979).
5. K. Kawasaki, T. Imaeda, and J. D. Gunton, in *Perspectives in Statistical Physics*, H. J. Raveché, ed. (North-Holland, Amsterdam, 1981), p. 203.
6. K. Binder, *Z. Phys. B* **43**:119 (1981); *Phys. Rev. Lett.* **47**:693 (1981).
7. K. Kaski, K. Binder, and J. D. Gunton, *J. Phys. A* **16**:L623 (1983); *Phys. Rev. B* **29**:3996 (1984).
8. S. A. Newlove and A. D. Bruce, *J. Phys. A* **18**:598 (1985).
9. A. D. Bruce, *J. Phys. C* **14**:3667 (1981).
10. J. D. Gunton, M. San Miguel, and P. Sahni, in *Phase Transitions and Critical Phenomena*, Vol. 8, C. Domb and J. L. Lebowitz, ed. (Academic, London, 1983), p. 263.
11. C. S. S. Murty and D. P. Landau, *J. Appl. Phys.* **55**:2429 (1984) and preprint.
12. K. Binder and D. P. Landau, *Phys. Rev. B* **30**:1477 (1984); M. S. S. Challa, D. P. Landau, and K. Binder, *Phys. Rev. B* (1986, in press).
13. A. B. Bhatia and N. H. March, *J. Chem. Phys.* **68**:4651 (1978); J. W. Cahn, *J. Chem. Phys.* **66**:3667 (1977); H. Nakanishi and M. E. Fisher, *Phys. Rev. Lett.* **49**:1565 (1982).
14. T. Ohta and K. Kawasaki, *Progr. Theor. Phys.* **58**:467 (1977); J. Rudnick and D. Jasnow, *Phys. Rev. B* **17**:1351 (1978).
15. M. E. Fisher, *Rev. Mod. Phys.* **46**:587 (1974); K. G. Wilson and J. Kogut, *Phys. Rept. C* **12**:77 (1974).
16. J. C. Le Gouillou and J. Zinn-Justin, *Phys. Rev. B* **21**:3976 (1980).
17. G. A. Baker, Jr. and J. M. Kincaid, *Phys. Rev. Lett.* **42**:1431 (1979).
18. G. A. Baker, Jr. and J. D. Johnson, *J. Phys. A* **17**:L275 (1984); *Phys. Rev. Lett.* **54**:2461 (1985).
19. D. Mukamel and S. Krinsky, *Phys. Rev. B* **16**:2313 (1977).
20. For reviews, see R. A. Cowley, *Adv. Phys.* **29**:1 (1980); A. D. Bruce, *Adv. Phys.* **29**:111 (1980); A. D. Bruce and R. A. Cowley, *Adv. Phys.* **29**:219 (1980).
21. E. Eisenriegler, *Phys. Rev. B* **9**:1029 (1974).
22. T. Schneider and E. Stoll, *Phys. Rev. B* **13**:1216 (1976); *Phys. Rev. Lett.* **31**:1254 (1973); *Ferroelectrics* **24**:67 (1980).
23. R. Morf, T. Schneider, and E. Stoll, *Phys. Rev. B* **16**:462 (1977).
24. T. W. Burkhardt and W. Kinzel, *Phys. Rev. B* **20**:4730 (1979).
25. H. Müller-Krumbhaar, *Z. Physik B* **35**:339 (1980).
26. P. D. Beale, S. Sarker, and J. A. Krumhansl, *Phys. Rev. B* **24**:266 (1981).
27. G. A. Baker, Jr., P. D. Beale, A. R. Bishop, K. Fesser, and J. A. Krumhansl, *Phys. Rev. B* **26**:2596 (1982).
28. L. D. Roelofs, G. Y. Hu, and S. C. Ying, *Phys. Rev. B* **28**:6369 (1983).
29. P. A. Bak, *Solid State Comm.* **32**:581 (1979).
30. B. Freedman, P. Smolensky, and D. Weingarten, *Phys. Lett. B* **113**:481 (1982).
31. I. Aviran, S. Goshen, D. Mukamel, and S. Shtrikman, *Phys. Rev. B* **12**:438 (1975).
32. M. J. Clouter, H. Kiefte, and C. G. Deacon, *Phys. Rev. B* (1986).
33. J. A. Tuszynski, M. J. Clouter, and H. Kiefte, *Phys. Lett. A* **108**:272 (1985).
34. M. E. Fisher, in *Critical Phenomena*, M. S. Green, ed. (Academic Press, New York, p. 1, 1971); for a recent review, see M. N. Barber, in *Phase-Transition and Critical Phenomena*, Vol. 8, C. Domb and J. L. Lebowitz, eds. (Academic Press, New York, p. 145, 1983).
35. D. P. Landau, *Phys. Rev. B* **13**:2297 (1976).

36. K. Binder and D. P. Landau, *Phys. Rev. B* **21**:1941 (1980).
37. M. Barma and E. Fisher, *Phys. Rev. B* **31**:5954 (1985); *Phys. Rev. Lett.* **53**:1935 (1984); **54**:2462 (1985).
38. K. Binder, ed., *Monte-Carlo Methods in Statistical Physics* (Springer, Berlin–Heidelberg–New York, 1979); *Applications of the Monte-Carlo Method in Statistical Physics* (Springer, Berlin, 1984).
39. K. Binder and D. P. Landau, *Surf. Sci.* **151**:409 (1985).
40. T. W. Burkhardt, private communication; T. W. Burkhardt and B. Derrida, preprint.
41. K. Binder, *Z. Phys. B* **61**:13 (1985).
42. M. J. Clouter, private communication.
43. E. Brézin, *J. Phys. (Paris)* **43**:15 (1982).
44. E. Barouch, B. M. McCoy, and T. T. Wu, *Phys. Rev. Lett.* **31**:1409 (1973).
45. K. Binder, *Phys. Rev. A* **20**:341 (1984).
46. C. N. Yang, *Phys. Rev.* **85**:808 (1952).
47. A. D. Bruce, *J. Phys. A* **18**:L873 (1985).